KINETIC STUDIES OF ISOPRENE REACTIONS WITH

HYDROXYL AND CHLORINE RADICALS

A Thesis

by

INSEON SUH

Submitted to the Office of Graduate Studies of
Texas A&M University
in partial fulfillment of the requirements for the degree of

MASTER OF SCIENCE

August 2000

Major Subject: Atmospheric Sciences

KINETIC STUDIES OF ISOPRENE REACTIONS WITH

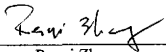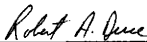# HYDROXYL AND CHLORINE RADICALS

A Thesis

by

INSEON SUH

Submitted to Texas A&M University
in partial fulfillment of the requirements
For the degree of

MASTER OF SCIENCE
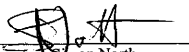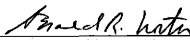
Approved as to style and content by:

Renyi Zhang	Robert A. Duce
(Chair of Committee)	(Member)
Simon North	Gerald R. North
(Member)	(Head of Department)

August 2000

Major Subject: Atmospheric Sciences

ABSTRACT

Kinetic Studies of Isoprene Reactions with

Hydroxyl and Chlorine Radicals.

(August 2000)

Inseon Suh, B.S. Seoul Women's University

Chair of Advisory Committee: Dr. Renyi Zhang

Kinetic studies of the isoprene oxidation reactions initiated by the hydroxyl radical OH and the chlorine atom Cl have been investigated using a fast-flow reactor in conjunction with chemical ionization mass spectrometry (CIMS) and using laser photolysis/laser induced fluorescence (LP/LIF) detection. Both the CIMS and LP/LIF techniques were employed to investigate the reaction of isoprene with OH. The rate constants for the OH-isoprene reaction were measured in a pressure range of 70 to 112 Torr using the CIMS approach, with values of (9.7 ± 1.0) x 10^{-11} to (10.5 ± 1.1) x 10^{-11} cm^3 $molecule^{-1}$ s^{-1} at 298 ± 2 K. The LP/LIF method was used to measure the pressure dependent rate constants in a pressure range of 0.5 to 20 Torr. A low pressure limiting termolecular rate constant, $k_o = (6.98 \pm 2.2)$ x 10^{-26} cm^6 $molecules^{-2}$ s^{-1} and a high pressure limiting rate constant, $k_1 = (1.04 \pm 0.04)$ x 10^{-10} cm^3 $molecules^{-1}$ s^{-1} at 295 K were obtained by fitting the measured rate constants according to the Troe expression. The CIMS approach allowed monitoring of the OH-isoprene adducts directly. The observed bimolecular rate constant for the reaction between the OH-isoprene adduct and O_2 was determined to be (2.8 ± 0.7) x 10^{-15} cm^3 $molecule^{-1}$ s^{-1} at 75.5 Torr.

In addition, the reaction of isoprene initiated by Cl atom has been studied, using the CIMS method. The reaction of isoprene with Cl proceeds via both the Cl addition to isoprene and hydrogen abstraction to form HCl. The pressure independent rate constant of $(4.0 \pm 0.3) \times 10^{-10}$ cm^3 molecule^{-1} s^{-1} for the Cl-isoprene reaction was obtained in a pressure range of 5 to 10 Torr. The branching ratio of $(17.7 \pm 3.2)\%$ for the reaction of Cl with isoprene was derived by monitoring the formation of HCl in accordance with the consumed Cl concentrations. Furthermore, the overall rate constant for the reaction between the Cl-isoprene adduct and O_2 was determined as $(1.0 \pm 0.3) \times 10^{-14}$ cm^3 molecule^{-1} s^{-1}, by modeling the reaction system in the experiments.

Hence, in this work we have developed experimental techniques for the isoprene oxidation reactions with the OH radicals and Cl atoms, which should provide insight for understanding of the photochemical oxidation of isoprene in the atmosphere.

ACKNOWLEDGMENTS

I would like to express my heartfelt thanks to Dr. Renyi Zhang, my advisor, for his guidance and support in this work. His advice and patience have provided this author with invaluable experience. Also, I am deeply grateful to Dr. Simon North for his advice, assistance, and patience during this work. Dr. Robert A.Duce was also very generous and helpful as member of my graduate committee. I am also grateful to Sean W. McGivern for providing experimental results and technical advice. I would like also to thank Wenfang Lei and Angela Clinkenbeard, members of the research group, for their assistance.

I would also like to acknowledge my family, Dongkun Suh, Eunjoo Nam, and Jongwan Suh for their continuous support, encouragement and love. Thanks are also extended to my friends for their support and encouragement. A special mention goes to Heejo Moon and Sangmi Han.

TABLE OF CONTENTS

viii

LIST OF FIGURES

LIST OF TABLES

CHAPTER I

INTRODUCTION

1-1. Statement of the Problem

Human activities are directly connected to the chemical processes in the troposphere, since many chemical species are emitted into the atmosphere from multiple sources. Primary air pollutants such as oxides of nitrogen (NO_x), and volatile organic compounds (VOCs), including hydrocarbons, are emitted into the urban and regional atmosphere from anthropogenic sources. For example, NO_x is produced from power plants, industry, and from automobiles, and VOCs are emitted from automobiles. In addition, some of the most important chemical compounds including VOCs are produced predominantly from vegetation.[1-4] The chemistry of atmospheric VOCs is important for understanding chemical processes occurring in the troposphere.[5,6] For example, the reactions of VOCs with oxides of nitrogen combined with temperature inversions in the troposphere and sunlight result in the formation of urban photochemical smog. This leads to the formation of ozone in rural and urban areas[7] as well as in the global troposphere[8]. They also play a role in acid deposition[9] and the greenhouse gas effect.[10]

Atmospheric VOCs are emitted into the troposphere from anthropogenic and biogenic sources.[1-2,11] For example, the annual emission rate of methane is ~ 155-240 Tg yr^{-1} from biogenic sources and ~350-375 Tg yr^{-1} from anthropogenic sources.[11] Isoprene (2-methayl 1,3-butadiene), one of the most abundant non-methane hydrocarbons[1-2], is

---

The style and format of this thesis follow *The Journal of Physical Chemistry*.

emitted from deciduous trees that emit about 1 % of the CO_2 fixed as isoprene, with a global averaged production rate of approximately 450 Tg yr^{-1}. The isoprene production is even higher than that of anthropogenic non-methane hydrocarbons in rural and remote areas.[12,13] In addition, isoprene has two double bonds, and is highly reactive with atmospheric oxidants such as hydroxyl radicals (OH), ozone, NO_3 (during nighttime), and halogen atoms. It significantly influences oxidation levels over large portions of the continental troposphere.[14]

In the troposphere there are two sources for ozone formation. One is the photochemical ozone formation from the atmospheric oxidation of methane, carbon monoxide, and other VOCs, and the other is downward ozone transported from the stratosphere.[8,15] Ozone is an important source for the formation of the hydroxyl radical OH, a key oxidizing species in the troposphere. Photolysis of ozone produces the excited oxygen atom $O(^1D)$[16] at wavelengths less than 290 nm[17]. The reaction of $O(^1D)$ with water vapor in the daylight leads to the formation of most OH radicals in the troposphere.[16,17] The production of OH radical is expected to be higher especially in the lower troposphere where the water vapor mixing ratio is high. The other sources of OH radicals are the photolysis of nitrous acid (HONO), formaldehyde, and other carbonyl compounds during daylight.[18] Since isoprene is mainly emitted in the day time from the vegetation, the reaction with the OH radical is considered to be the dominant channel for the removal of isoprene in the troposphere. Therefore, a precise and complete understanding of the isoprene oxidation mechanism initiated by the hydroxyl radical is important to understand the urban and regional air quality.[19-23]

The reaction between isoprene and OH occurs almost entirely by OH addition to the

>C=C< bonds, yielding four possible OH-isoprene adduct isomers.[24] The OH radical addition at the 1- or 4- position of conjugated dienes mainly forms the β-hydroxyalkyl radical, which can isomerize to form the thermodynamically favored allylic β(or δ-)-hydroxyalkyl radical (HOCH$_2$ (CH$_3$)CH=CH$_2$↔HOCH$_2$C(CH$_3$)=CH H$_2$).[25-26] In the troposphere, the various hydroxyl-substituted allyl-type radicals react exclusively with oxygen molecules to form the β(or δ-)-hydroxyalkyl peroxy radicals. In the presence of nitric oxide NO, these hydroxyalkyl peroxy radicals form either the hydroxyalkoxy radicals and NO$_2$ or the hydroxyalkyl nitrate. Figure 1 shows a mechanistic diagram for the formation of the OH-isoprene adducts and their corresponding peroxy radicals. The dominant tropospheric reaction of the β-hydroxyalkoxy radicals is decomposition, leading to the formations of HCHO plus methyl vinyl ketone [CH$_3$C(O)CH=CH$_2$] or HCHO plus methacrolein[CH$_2$=C(CH$_3$)CHO], depending onto which >C=C< bond the OH radical adds.[25,26] The minor channel of the β-hydroxyalkoxy radicals formed after the OH radical addition to isoprene is isomerization.[25,26]

Several studies have been carried out to determine the oxidation reactions of isoprene initiated by OH[5,24] either in a kinetic or mechanistic way. Laboratory experiments using the smog chamber approach have identified and quantified the major reaction products, including methacrolein, methyl vinyl ketone, formaldehyde, 3-methylfuran and organic nitrates.[25,27-33] The rate constants for the reaction of isoprene with OH have been investigated using both relative rate method[34-36] and absolute rate measurement.[37-39] The temperature dependent rate constants of isoprene with OH have been reported,[34-39] indicating a weak negative dependence for the OH addition. Most of those studies were conducted at 760 Torr, except for the work by Kleindlenst et al.,[37]
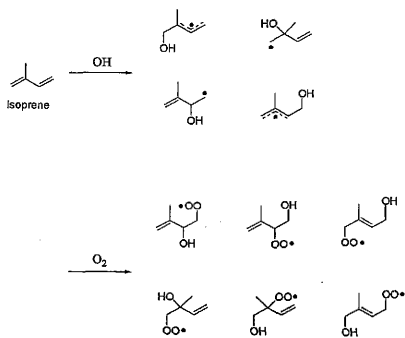
Figure 1. A mechanistic diagram for the reactions of OH with isoprene and the OH-isoprene adduct with O_2

which was performed at 50 and 200 Torr. The latter authors conclude that there is no significant pressure dependence for this reaction over this pressure range. The high-pressure limit rate constant of 1.01×10^{-10} cm^3 molecule^{-1} s^{-1} has been recommended at 298K and 760 Torr.[40] Although the addition reaction such as OH addition to isoprene is expected to show a pressure dependence, the reaction in the low pressure region has not been well known. Recently, Stevens et al.[39] reported the rate constant of isoprene with OH, with a value of 1.09×10^{-10} cm^3 molecule^{-1} s^{-1} at 2 Torr of helium, suggesting that the high pressure limit is already reached at this condition. In addition, Jenkin et al.[41] has investigated the kinetics of the peroxy radical permutation reactions from the OH-initiated oxidation of isoprene.

At present, direct experimental data concerning the intermediate processes of the oxidation reactions of isoprene are very limited. There are few experimental studies available on the chemistry of the radical intermediates. The detailed reaction mechanism and pathways of the isoprene reaction system have not been clearly identified. Absolute or relative rate constants between the reactions of OH-isoprene adduct with O$_2$ and the subsequent reactions of the β-hydroxyalkyl peroxy and β-hydroxyalkoxy radicals are currently not available. Our understanding of the atmospheric oxidation mechanism of isoprene is primarily based on the environmental chamber investigations that identify the final products of the reactions.

In addition, there are some studies to incorporate the results from the laboratory studies into computer models to develop atmospheric oxidation mechanisms for isoprene.[26,42,43] Clearly, there is a need for an accurate and complete knowledge of the

atmospheric chemistry of isoprene in order to understand and elucidate air pollution in urban and regional environments.

In addition to the hydroxyl radical, there are also several other atmospheric oxidants, such as ozone, nitrate radical (NO_3), halogen atoms and their oxides. The oxidation by the OH radical is clearly the most important one among the oxidants, but ozone, NO_3, halogen atoms and their oxides can also react with isoprene and may in some cases make a larger contribution to the oxidation rate than OH radicals.[44] There is increasing evidence that the Cl atoms may be important for the tropospheric chemistry in the marine boundary layer and in coastal region.[45-48] Field measurements of the relative degradation rates of saturated hydrocarbons show significant deviation from what can be explained by the OH radical.[49-51] The high concentration of chlorine and bromine atoms have been related to the depletion of surface ozone during the arctic spring.[49,50] Chlorine atoms are highly reactive with a variety if organic and inorganic compounds. Relatively small concentrations can compete with the OH radical, ozone, and NO_3 in determining the lifetime of VOCs, although there is evidence that chlorine atoms cannot be compared with OH for the oxidation of organics on a global scale.[52,53] Reactive chlorine is produced in the atmosphere both as a consequence of direct emission and of multiphase chemical processes.[54] There are four major sources of reactive chlorine such as oceanic and terrestrial biogenic emissions, sea salt production and dechlorination, biomass burning, and anthropogenic emissions. The main source of chlorine atoms in the atmosphere may come from sea salt reactions, based on a variety of field, modeling and laboratory studies. Reactive chlorine compounds, including Cl_2, are generated by the heterogeneous reaction of sea salt aerosols with nitrogen oxides[55] and detected at concentration up to ~ 150 ppt in

coastal marine areas.[56,57] and in the Arctic at polar sunrises.[58] Cl_2 is expected to photolyze rapidly at dawn, providing reactive chlorine atoms. The peak concentration of chlorine atoms is estimated to be $\sim 10^3 - 10^5$ molecule cm^{-3}.[56-60] Especially, reactive chlorine atoms can play a significant role in the oxidation of isoprene during early morning in the marine boundary layer and coastal regions. The atmospheric oxidation of some VOCs can be important at the Cl-atom concentration of 5×10^3 molecule cm^{-3}, compared to an OH concentration of 5×10^5 molecule cm^{-3} in the early morning hours.[61]

Recent studies have also shown that isoprene is emitted by phytoplankton in seawater.[62-66] It is expected that the interaction of isoprene with chlorine atoms occurs rapidly in daylight as well as with OH and O_3 and with NO_3 at nighttime. This indicates that the reactions of hydrocarbons with Cl atoms can be an essential oxidation route in both the regional and marine atmosphere.

Several laboratory studies have investigated the kinetics and mechanisms of the oxidation reactions of isoprene initiated by Cl atoms. The rate constants have been investigated, using both a relative rate method [67-69] and an absolute rate method[70,71] The pressure dependence of the Cl-isoprene reaction has been investigated in the pressure range of 0.1 to 760 Torr.[67,70,71] Some of those studies have also identified the reaction products[67-69,71], including CO, CO_2, formyl chloride, formic acid, methyl-glyoxal, and hydrogen chloride. Other likely products of the isoprene reactions include α,β–unsaturated carbonyls (methyl vinyl ketone and methacrolein)[67,68] In addition, the branching ratio for the reaction of isoprene with Cl atoms has been investigated in the temperature range of 230-320 K.[71] At present, however, there are some controversies regarding the initial reaction of isoprene with chlorine atoms. For example, Notario et

al.[70] and Bedjanian et al.[71] report a rate constant of $(3.6 \pm 0.2) \times 10^{-10}$ cm^3 molecule^{-1} s^{-1} for the reaction of isoprene with Cl atom, which is 21 % lower than the rate constant reported by Ragains and Finlayson-Pitts[67]. There is also a disagreement in the reported pressure dependence. The work by Notario et al.[70] and Bedjanian et al.[71] suggested that this reaction is pressure independent in a range of pressure between 0.3 Torr and 760 Torr, in contrast to the earlier findings by Ragains and Finlayson-Pitts.[67]

In this thesis, laboratory experiments are presented to investigate the oxidation reaction of isoprene initiated by OH and Cl radicals, using two complementary experimental techniques: chemical ionization mass spectrometry (CIMS) and Laser Photolysis / Laser Induced Fluorescence (LP/LIF). The results provide insight into the atmospheric oxidation mechanism of isoprene.

1-2. Organization of the Thesis

The background and current literature are summarized in Chapter I related to the oxidation reactions of isoprene initiated by the hydroxyl radical and chlorine atom. In Chapter II, experimental methods using chemical ionization mass spectrometry (CIMS) for investigating the reaction of isoprene initiated by OH are presented. In Chapter III, the fall-off regime for the reaction of isoprene with the OH radical has been investigated using Laser Photolysis Laser Induced-Fluorescence (LP/LIF). The reactions of isoprene with Cl have also been studied using CIMS and are presented in Chapter IV. The results and discussion are presented in each Chapter II, III, and IV. Finally, concluding remarks are given in Chapter V.

CHAPTER II

OH-ISOPRENE REACTION STUDIED USING CIMS

In chapter II, we report kinetic studies of isoprene reactions initiated by the hydroxyl radical OH, using a fast–flow reactor coupled to chemical ionization mass spectrometry (CIMS) detection. The rate constants for the reaction of isoprene with OH have been measured in the pressure range of 70 to 120 Torr and at 298 ± 2 K. We also present direct observations of the OH-isoprene adduct based on ion-molecule reactions using the CIMS method. The OH-isoprene adduct was used to elucidate the reaction mechanism and to extract the rate constant between OH and isoprene. By monitoring the temporal evolution of the OH-isoprene adduct in the absence and presence of oxygen molecules, an overall rate constant between O_2 and OH-isoprene adduct has been determined.

2-1. Experimental Procedure

Reactor and Flow Conditions

A fast flow reactor, connected to chemical ionization mass spectrometry (CIMS) detection, was used to study the kinetics of reaction between isoprene and hydroxyl radicals. The configuration of the experimental setup is shown Figure 2. The flow reactor was constructed of precision-bore Pyrex tubing 2.45 cm in internal diameter and 60 in long. The inlet of isoprene is through the movable injector consisting of a 3.2 mm o.d. Pyrex tube which has a fan-shaped Teflon device on the tip of the injector to enhance
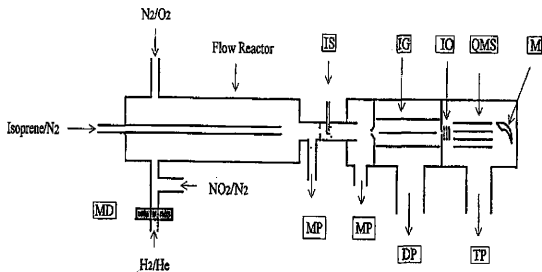
Figure 2. Schematic diagram of the fast-flow reactor/CIMS system: DP = diffusion pump, IG = ion guide, IO = ion optics, IS = ion source, M = multiplier, MD = microwave discharge, MP = mechanical pump, QMS = quadrupole mass spectrometer, and TP = turbo molecular pump

mixing of the reactants in the flow reactor. To check the flow system the chemiluminescence reaction was performed,[72]

$$O + NO_2 \rightarrow O_2 + NO + h\nu \tag{1}$$

This reaction visualized the flow pattern of the reactants in the flow reactor. It showed the homogeneous mixing of the reactants both in the radial and axial directions. In these experiments, oxygen atoms were generated by a microwave discharge and then injected into the flow reactor through an upstream side arm inlet and then mixed with NO_2 added through the injector. Under the experimental conditions reported in this work we observed homogeneously well-mixed green chemiluminescent glow from the reaction of O with NO_2 a few centimeter downstream of the tip of the injector. All inner surfaces where the flow reactor exposed to OH were coated with a halocarbon wax to reduce the wall loss of the OH radicals. A main carrier gas, nitrogen in the range of 1 to 3 STP l min^{-1} flowed into the flow reactor through an entrance port in the rear of the flow reactor. Typical flow velocity in the flow reactor ranged from 1400 to 1900 cm s^{-1}. The pressure in the flow reactor was adjusted between 70 and 120 Torr and all experiments were performed at 298 ± 2 K. The flow reactor was evacuated by a high capacity mechanical pump with 1000 l min^{-1}. Two capacitance manometers of 10 and 1000 Torr full scale monitored pressures in the flow reactor.

The characteristic of the flow in the reactor is determined by the Reynolds number $Re = 2au\rho/\mu$, where a is the internal radius of the flow reactor, ρ the density of the gas, u the flow velocity, and μ the viscosity coefficient of the gas.[73] For a turbulent flow the range of the Reynolds number is over 2000. A laminar flow is normally developed at Re < 2000. The distance for a fully developed laminar flow can be estimated

according to the expression of $l = 0.115aRe$.[74]   Our experimental conditions had typical values in a range of 2315 and 3500 for the Reynolds number. The mixing time for OH and isoprene can be described by $t_{mix} = a_2/(5D)$.[75]

<u>Ion Sources and the CIMS Detection</u>

Reactants and products from the flow reactor were introduced into the ion-molecule reaction region through an orifice of 10-mm diameter. A mechanical pump was used to evacuate this region to a pressure of 1-10 Torr. The CIMS detected the reactants and products of the isoprene reactions. A corona discharge at high voltage (-5 kV) generated positive or negative reagent ions. For SF_6^- reagent ions, a small amount of SF_6 was added to a He carrier flow (about 2 slpm at STP) and passed through the discharge. The O_2^+ or H_3O^+ reagent ions were produced by passing the He carrier flow through the discharge and then adding a small amount of H_2O or O_2 downstream. A small portion of the ion/gas flow from the ion source was drawn into the next vacuum stage through a 0.5-mm orifice. In our experiments, an electrostatic ion guide recently developed was used for efficient detection of CIMS.[76,77] Ions were efficiently transported to another orifice guided to the quadrupole mass analyzer. A diffusion pump and a turbomolecular pump evacuated the chamber consisting of the mass spectrometer and the ion guide, respectively. We achieved highly efficient ion transportation and preferential ion-molecule separation, using the ion guide. This device removes neutral molecules, passing two pumping systems.[76,77] Detection sensitivity of the present CIMS system was generally in the range of 10^7 to 10^8 molecules cm^{-3} with a S/N ratio of unity for a one second integration time, independent of the pressure. Thus it allows us to monitor the

intermediates or trace species formed during the isoprene oxidation reactions with high detection sensitivity.

Isoprene and OH Preparation

Two sources of isoprene (Aldrich 99.5%) were used in these experiments. First, isoprene flowed through a bubbler at the dry ice/acetone temperature along with N_2 gas and was added into the flow reactor in a range of 0.1 to 10 cm^3 min^{-1} at STP. It was further diluted in the main nitrogen carrier flow. We calibrated isoprene in the flow reactor according to the vapor pressure expression of pure isoprene of log P = 7.85 - 1511.41/T and the dilution factor of the isoprene flow. We also volumetrically prepared a 1 to 5% isoprene mixture with He in a 2-liter glass bulb. The isoprene mixture was introduced into the flow reactor by a 10-sccm flow meter. Calibration of isoprene using the two methods agreed within 5%. The concentrations of isoprene in the flow reactor were regulated in the range of 3 x 10^{11} to 5 x 10^{12} molecule cm^{-3}, which were at least a factor of 10 higher than the OH concentration to ensure the pseudo-first-order kinetic assumption. O_2^+ reagent ions were used to detect isoprene as the de-protonated [M- H]$^+$, the parent [M]$^+$, or the protonated [M + H]$^+$ isoprene ions, according to the ion-molecule reaction

$$O_2^+ + C_5H_8 \rightarrow C_5H_8^+ (C_5H_7^+ \text{ or } C_5H_9^+) + \text{products.} \qquad (2)$$
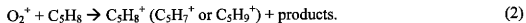
The ion-molecule reaction rate constant for reaction (2) has not been measured yet. Figure 3 represents a CIMS calibration of isoprene in the two different methods.
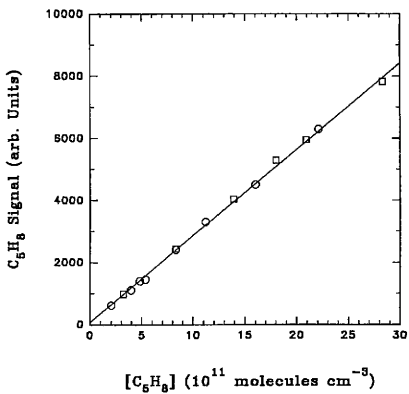
Figure 3. CIMS calibration of isoprene using two different methods (the bubbler method, open squares: the bulb method, open circles)

The mass spectrometer signals of isoprene were linear in the range of concentrations used in this work.

Hydroxyl radicals were generated *in situ* according to the fast titration reaction[16]

$$H + NO_2 \rightarrow NO + OH \qquad (3)$$

where the rate constant for the reaction is $k_3 = 1.3 \times 10^{-10}$ cm^{3}molecule^{-1} s^{-1}. Hydrogen atoms were produced by flowing a 3% H_2/He mixture through a microwave discharge at about 0.5 cm^3 min^{-1} at STP. Then an excess 3% NO_2/ N_2 mixture was added to titrate the H atoms. OH was detected as the negative ion mode using the SF_6^- reagent ions,

$$OH + SF_6^- \rightarrow OH^- + SF_6 \qquad (4)$$

where the rate constant for this reaction is $k_4 = 2 \times 10^{-9}$ cm^3 molecule^{-1} s^{-1} [78]. The concentrations of OH radicals were calibrated by two methods. First, we monitored the relative signal intensities between OH and NO_2 and then calibrated NO_2. The OH concentration was obtained by using the relation,

$$[OH] = k_3 S_{OH}[NO_2]/(k_6 S_{NO2}) \qquad (5)$$

where k_6 is the ion-molecule reaction rate constant between NO_2 and SF_6^-, with a value of $k_6 = 1.4 \times 10^{-10}$ cm^3 molecule^{-1} s^{-1}.[79]

$$NO_2 + SF_6^- \rightarrow NO_2^- + SF_6 \qquad (6)$$

For ensuring the validation of Equation (5) the OH calibration experiments were performed under the condition that the mass spectrometer was operated at low resolution to minimize the mass discrimination. This approach is the main method of obtaining the concentration of hydroxyl radicals in this experiment. Another way to calibrate OH is to convert all of the OH into HNO_3 followed by HNO_3 calibration in the mass spectrometer. The ion-molecule reaction to detect nitric acid (HNO_3) is

$$HNO_3 + SF_6^- \rightarrow HNO_3 \bullet F^- + SF_6 \qquad (7)$$

where the rate constant is $k_7 = 2 \times 10^{-9}$ cm^3 molecule^{-1} s^{-1}. A 60 wt % HNO$_3$ solution in an ice-water bath was used to determine the HNO$_3$ concentration in the flow reactor. Both approaches yielded OH concentrations within 50 %. We estimated the initial concentrations of OH in the flow reactor in the range of 5×10^9 to 7×10^{10} molecule cm^{-3}.

For both OH and isoprene the mass spectrometer signals were found to be linear over the range of concentrations used in this work.

Mass flow meters (Tylan General) were used to monitor all the flows introduced into the flow reactor. The following gases were used without further purification: He (99.999%), O$_2$ (99.994%), H$_2$ (99.999%), and NO$_2$ (99.5%).

2-2. Results and Discussion

Isoprene Reaction with OH Radicals

The kinetic studies of the reaction of isoprene initiated by hydroxyl radicals were investigated under the pseudo-first order approximation. It is believed that addition of OH to isoprene leads to the formation of the OH-isoprene adduct. The observed first order loss rate coefficients (k^I, s^{-1}) were derived directly based on the plot of the decay of the OH radical signals as a function of the reaction distance in the presence of excess isoprene.

$$OH + C_5H_8 \rightarrow C_5H_8OH \qquad (8)$$
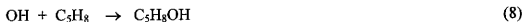
The Reynolds number, *Re*, characterizes the nature of the flow. If the Reynolds number is less than 2000, the experimental flow is laminar. Turbulence starts to build at Re greater than about 2000. Under laboratory conditions (i.e. the pressure between 70 to 120 Torr and flow velocities between 1400 and 1900 cm s^{-1}) the Reynolds number *Re* was calculated to be in the range of 2315 to 3500. When the turbulent flow conditions were achieved in the flow reactor, the effect of wall loss of reactants and products would be minimal. The apparent rate constants obtained from the observed first-order loss rate coefficient are less than 10 % different from the true rate constants.[72,80-82] Thus we obtained the bimolecular rate constant of the OH-isoprene reaction directly from the observed first order rate coefficients under the turbulent flow conditions. In additions, we measured that the first-order rate of OH on the flow reactor surface was less than 1 s^{-1}.

The observed first order loss rate coefficients (k^I, s^{-1}) were derived directly based on the plot of the decay of the OH radical signals as a function of the reaction distance. Figures 4a presents the pseudo-first order decay of OH in the presence of isoprene. The slope of the plots of the logarithm of the OH signal vs. reaction time corresponds to the observed first-order rate coefficients (k^I). The secondary reactions in our experiments were not expected to intercede k^I because those plots were linear. The experimental conditions were 103.1 Torr and Re = 3436. The initial concentration of OH was estimated to be 9.4 x 10^9 molecule cm^{-3} and the isoprene concentrations were varied between 3.8 x 10^{11} and 10.2 x 10^{11} molecule cm^{-3}. The background signals of OH (17 m/e) in these experiments were subtracted from all the points shown in the figures. Figure 4b shows the plot of the first-order coefficient as a function of isoprene concentration. The slope of the fit to the experimental data provides an effective bimolecular rate constant for the

reaction of isoprene with OH radicals with a value of $(10.5 \pm 1.1) \times 10^{-11}$ cm^3 molecule^{-1} s^{-1}. The linear pseudo-first order decays for OH data in figure 4a and figure 4b indicate that the mixing of the reactants in our experiments was effectively achieved.

The rate constant for the reaction of isoprene with OH was measured at different flow reactor pressure, ranging from 70 to 120 Torr. A summary of the rate constants determined near room temperature (298 ± 2 K) is in Table 1. Figure 5 shows that the rate constant is nearly pressure independent in the pressure range of 70 to 120 Torr. The measured rate constant ranged from $(9.7 \pm 1.0) \times 10^{-11}$ to $(10.5 \pm 1.1) \times 10^{-11}$ cm^3 molecule^{-1} s^{-1}. The measured rate constants in Figure 5 agreed well with the previous data in the literature.[56,57] The quoted uncertainty indicated the scatter in the data at the one standard deviation level and systematic errors are not included. We estimated about ± 15 % systematic error in the present data, which were from experimental measurements of gas flows, temperature and pressure and from the plug flow approximation The kinetic studies for the low-pressure region were explored by laser photolysis/laser-induced fluorescence (LP/LIF), described in Chapter III.

Observation of OH-Isoprene Adduct

We observed directly the OH-isoprene adduct of the reaction between isoprene and OH radicals, using the CIMS method. The mass spectrometer only detects the mass of ions. It does not differentiate isomers resulting from the reaction of isoprene initiated by OH radicals. From the previous mechanistic studies, the addition of OH to the double
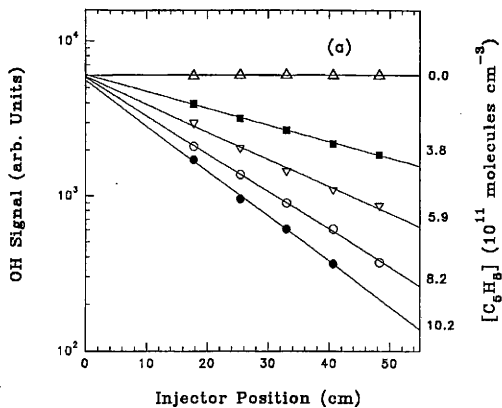
Figure 4a. Variation of OH signal as a function of injector distance for various
concentration of isoprene. A background signal of 240 was subtracted
from all the data shown in the figure
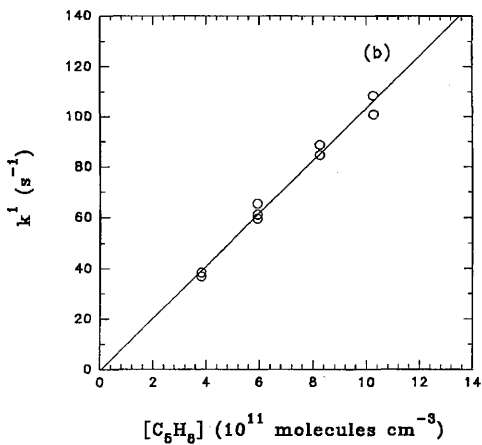
Figure 4b. First-order loss rate coefficient k^I as a function of isoprene concentration. Experimental conditions are: P = 103.1 Torr, U = 1498, Re = 3436, and $[OH]_o$ = 9.4 x 10^9 molecule cm^{-3}

Table 1. Summary of reaction rate constants for OH plus isoprene determined by using the CIMS method

T (K)	P (Torr)	U (cm s^{-1})	*Re*	K (cm^3 molecule^{-1}s^{-1})
298 ± 2[a]	72.7	1561	2315	(9.7 ± 0.8) x 10^{-11}
	80.8	1511	2493	(9.7 ± 0.6) x 10^{-11}
	91.2	1530	2848	(10.2 ± 0.9) x 10^{-11}
	103.1	1498	3151	(10.5 ± 1.1) x 10^{-11}
	112.7	1493	3436	(10.2 ± 0.9) x 10^{-11}
298[b]	760			7.4 x 10^{-11}
299[c]	50,200			(9.3 ± 1.5) x 10^{-11}
299 ± 2[d]	760			(9.6 ± 0.4) x 10^{-11}
298[e]	760			(10.1 ± 0.3) x 10^{-11}
298[f]				9.7 x 10^{-11}

[a]This work, [34]Reference, [35]Reference, [36]Reference, [37]Reference, [38]Reference
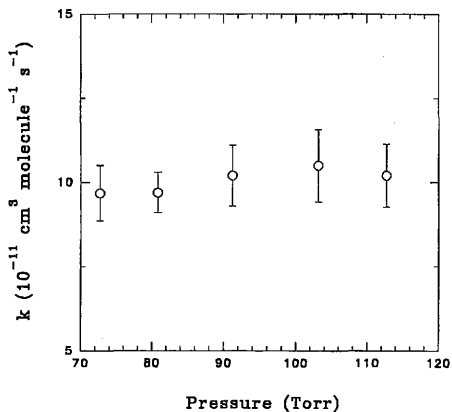
Figure 5. Bimolecular rate constant for the reaction of isoprene with OH as a function of pressure. The experimental conditions are: U = 1400 to 1900 cm s^{-1}, Re = 450 to 3500, $[OH]_o$ = 5.0 x 10^9 to 6.0 x 10^{10} molecule cm^{-3}, and $[C_5H_8]_o$ = 2.0 x 10^{11} to 6.0 x 10^{12} molecule cm^{-1}

bonds of isoprene may result in the formation of four possible isomeric radicals (Figure 1). According to *ab initio* calculations the more energetically favorable channels were via OH addition to the 1- and 4-positions, by as much as 12 kcal mol^{-1} [83], consistent with experimental product studies [27-33] for this reaction system.

Because the CIMS is incapable of discriminating the various isomers formed in our experiments, we referred to the product from the reaction of isoprene with OH as "the OH-isoprene adduct" with mass 85 and atomic composition C_5H_8OH. The positive reagent ions of O_2^+ or H_3O^+ were used for detection of the adduct by the following ion-molecule reaction,

$$O_2^+ + C_5H_8OH \rightarrow C_5H_8OH^+ + O_2 \qquad (9)$$

or

$$H_3O^+ + C_5H_8OH \rightarrow C_5H_8OH^+ + H_2O + H \qquad (10)$$
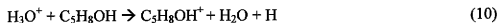
The rate constants for those reactions have not been measured yet, but they are likely to be exothermic.[84] The positive O_2^+ reagent ions were mainly used for the detection of the adduct in this work.

We took several procedures to positively verify that the signals detected at *m/e* = 85 were attributable to the OH-isoprene reaction, rather than to secondary ion-molecule reactions. First, we observed that the signal at mass 85 disappeared either when the isoprene flow into the reactor was stopped or when the microwave discharge for

dissociating the hydrogen molecules was turned off. These steps confirmed that the signal

at mass 85 was related to the OH-isoprene reaction. Second, we monitored the evolution

of the signal at mass 85, when the isoprene was introduced through the movable injector.

The results are shown in Figure 6. The temporal profile of the OH-isoprene adduct was

obtained in experimental conditions with $P = 75.5$ Torr, $Re = 2243$ and $U = 1452$ cm s^{-1}.

The initial concentrations of OH radicals and C_5H_8 were estimated to be of 4.0 x 10^{10}

molecule cm^{-3} and of 7.5 x 10^{11} molecule cm^{-3}, respectively. Figures 6 (a) and (b) show

that the signal of the OH-isoprene adduct rises in accordance with OH disappearance.

The OH decay (solid curve) in Figure 6(a) corresponds to an effective bimolecular rate of

9.3 x 10^{-11} cm^3 molecule^{-1} s^{-1}. As is shown in Figure 6(b), OH-isoprene adduct signals

gradually increase when the reaction distance increase. We have performed numerical

calculations to simulated the temporal profile of the OH-isoprene adduct with a simple

model. Table 2 lists the reactions and rate constants used in this simulation. The model

input included the initial concentrations of OH, isoprene, and all other precursors.

Table 2. Summary of the chemical reactions used in computer simulations for the system involving OH and isoprene

Reaction	k (cm^3 molecule^{-1} s^{-1})
$C_5H_8 + OH \rightarrow C_5H_7OH$	1.0×10^{-10} [a]
$OH + NO \rightarrow HONO$	1.4×10^{-12}
$OH + NO_2 \rightarrow HNO_3$	2.9×10^{-12}
$NO_2 + C_5H_8 \rightarrow$ products	1.8×10^{-19}
$OH + HO_2 \rightarrow H_2O + O_2$	1.1×10^{-10}

Rate constants are from Refs 16 and 20 at 298 K and 76 Torr, except noted otherwise. [a]From this work.
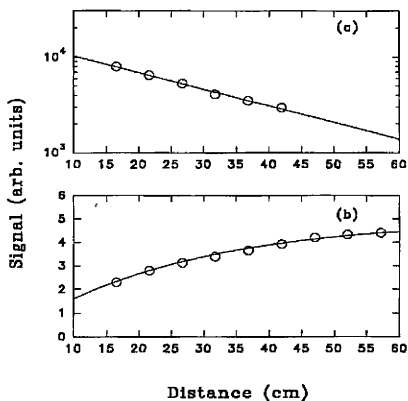
Figure 6. Variation of the OH (a) and OH-isoprene adduct (b) signals as a function of reaction time. The solid curves are from model calculations (see text). Experimental conditions are: $P = 33.6$ Torr, $U = 1434$ cm s^{-1}, $Re = 983$, $[OH]_o = 4.8 \times 10^{10}$ molecule cm^{-3}, and $[C_5H_8]_o = 7.5 \times 10^{11}$ molecule cm^{-1}

The rate constant of the reaction (8) was varied to fit the observed OH-isoprene adducts signals to the calculated temporal profile. The values from both channels are consistent within the uncertainty of the experiments. Note that the results of the OH decay and adduct growth shown in Figure 6 were corrected separately because either negative or positive reagent ions were used for the detection of OH or the adduct, respectively. The solid line in Figure 6(b) corresponds a best fit of the observed OH-isoprene adduct formation. An effective bimolecular rate constant of 9.1×10^{-11} cm^3 $molecule^{-1}$ s^{-1} was inferred. The rate constants of measured from the OH decay and fitting the formation of the OH-isoprene adduct are in good agreement for all experimental conditions. Hence, we believe the secondary reactions of the OH-isoprene adduct with NO or NO_2 were not important in our reaction system. In addition, heterogeneous loss of the OH-isoprene adduct on the surfaces of the flow reactor also appeared to be minimal in our experiments.

OH-Isoprene Adduct Reaction with O_2

We have further examined the temporal evolution of the OH-isoprene adduct in the presence of oxygen molecules. As mentioned above, the various hydroxy allylic radicals are expected to react solely with O_2 to form β(or δ-)-hydroxyalkyl peroxy radicals.

$$C_5H_8OH + O_2 \rightarrow C_5H_8OHO_2 \qquad (11)$$

In order to derive a rate constant between the OH-isoprene adduct and O_2, first, we monitored the temporal profile of the OH-isoprene adduct without adding O_2 when the injector was successively pulled upstream to increase the reaction time. A

bimolecular rate constant of the OH-isoprene reaction was obtained by fitting the measured OH-isoprene adduct data to simulated profile, using the reaction mechanism outlined in Table 3, along with estimated concentrations of the reactants. This rate constant was included to numerical model for the reaction of the OH-isoprene adduct with O_2. The experiment was then repeated under the same conditions with added O_2 in the flow reactor with a known concentration. We obtained the rate constant for the reaction of the OH-isoprene adduct with O_2 by fitting the solid line passing through the measured the OH-isoprene signals. In our study, the potential reaction between H atoms and O_2 was not important because an excess of NO_2 was used to completely convert H atoms into OH before entering the flow reactor. This was verified from the observation of the invariant OH signal when O_2 was added into the reactor.

The temporal evolution of the OH-isoprene adducts with (open squares) and without O_2 (open circles) is shown in Figure 7. The experiments were conducted at 75.5 Torr and at various concentration of isoprene and O_2. The initial concentration of OH radicals was estimated about 4.0×10^{10} molecule cm^{-3}. In Figure 7(a), the open squares stand for the OH-isoprene signals when the initial concentration of isoprene is 8.2×10^{11} molecule cm^{-3}, with the added O_2 concentration of 4.4×10^{15} molecule cm^{-3}. The bimolecular reaction rate for the formation of the OH-isoprene adduct in the absence of O_2 was obtained by fitting the solid line passing through the measured data (open circles), with a value of 9.1×10^{-11} cm^3 molecule^{-1} s^{-1}. This rate constant and the simulated profile for the OH-isoprene adduct in the presence of O_2 (short dashed curve) was used to determine an effective bimolecular rate constant for the reaction of the OH-isoprene adduct and O_2. The fit of the data corresponded to a value of 2.8×10^{-15} cm^3 molecule^{-1} s^{-}

[1]. Figure 7(b) has similar experimental conditions except higher concentration of isoprene of 6.3 x 10^{12} molecule cm^{-3} and higher O$_2$ concentration of 6.5 x 10^{15} molecule cm^{-3}. The bimolecular rate constants for the reaction of isoprene with OH (solid curve) and for OH-isoprene adduct with O$_2$ (short dashed curve) were determined to be 9.9 x 10^{-11} and 2.8 x 10^{-15} cm^3 molecule^{-1} s^{-1}, respectively. As is seen in the Figure, the OH-isoprene adduct profile at higher O$_2$ concentration (short dashed curves) indicates less production of the OH-isoprene adduct. In the presence of O$_2$, the production of the OH-isoprene adduct is reduced. This occurs because of the direct reaction between the OH-isoprene adduct and O$_2$ to form hydroxyalkyl peroxy radicals. OH addition to the terminal position of the unsaturated double bond results in allylic resonance, and OH addition to the inner position of the unsaturated double bond results in primary radicals.[23,25] Addition of O$_2$ to the adduct could yield the formation of six peroxy radicals in Figure 1.

The measured rate constant between the OH-isoprene adduct and O$_2$ at 75.5 Torr is (2.8 ± 0.7) x 10^{-15} cm^3 molecule^{-1} s^{-1}. This value represents an average of at least ten measurements at various isoprene and O$_2$ concentrations. The errors are indicative of the scatter in the data at the one standard deviation level. We believe that this rate constant corresponds most likely to the overall rate constants between the OH-isoprene adduct and O$_2$, rather than to individual isomeric radicals. For aromatic compounds, such as benzene and toluene, the oxidation reaction rate constants of hydroxylcyclohexadienyl and alkyl substituted hydroxylcyclohexadienyl with O$_2$ are on the order of 10^{-16} cm^3 molecule^{-1} s^{-1} [85], smaller than that of our results. On the contrast, it has been reported that the reaction rates between allyl (C$_3$H$_5$) radical and O$_2$ to form the allyl peroxy (CH$_2$=CHCH$_2$O$_2$) are 4 x 10^{-13} cm^3 molecule^{-1} s^{-1} at 380 K and 50 Torr [86] and (6 ± 2) x 10^{-13} cm^3 molecule^{-1} s^{-1} at

296 ± 2 K and 740-800 Torr.[87] We estimate a systematic error of about $\pm$ 50% for this reaction in the present data. The source of errors include uncertainty associated with detection and modeling of the OH-isoprene adduct, in addition to experimental uncertainties such as in the measurements of gas flows, temperature, and pressure.

Table 3. Summary of the chemical reactions used in computer simulations for the system involving OH, isoprene, and O_2

Reaction	k (cm^3 molecule^{-1} s^{-1})
C_5H_8 + OH → C_5H_7OH	$1.0 \times 10^{-10 \, b}$
C_5H_8OH + O_2 → $C_5H_8OHO_2$	$2.8 \times 10^{-15 \, b}$
OH + OH → H_2O_2	1.2×10^{-12}
OH + H_2O_2 → H_2O + HO_2	1.8×10^{-14}
OH + NO → HONO	1.4×10^{-12}
OH + NO_2 → HNO_3	2.9×10^{-12}
NO_2 + C_5H_8 → products	1.8×10^{-19}
$C_5H_8OHO_2$ + NO → C_5H_8OHO + NO_2	9.0×10^{-12}
C_5H_8OHO + O_2 → HO_2 + $C_5H_8O_2$	7.6×10^{-15}
C_5H_8OHO → CH_2OH + O_2 + products	1.5×10^{5}
CH_2OH + O_2 → HCHO + HO_2	9.8×10^{-12}
HO_2 + NO → OH + NO_2	8.5×10^{-12}
OH + HO_2 → H_2O + O_2	1.1×10^{-10}

[a] Rate constants are from Refs 16 and 24 at 298 K and 76 Torr, except noted otherwise. [b] From this work.
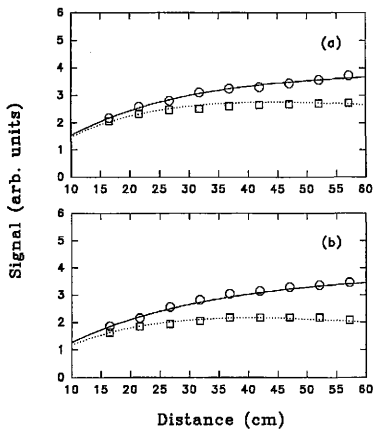
Figure 7. Production of the OH-isoprene adduct as a function of the reaction time in the absence (open circles) and presence (open squares) of O_2. The solid and short dashed curves are from model calculations (see text). $[OH]_0 = 4.8 \times 10^{10}$ molecule cm^{-3}. The initial concentrations of C_5H_8 and O_2 are: (a) 8.2×10^{11} and 4.4×10^{15} molecule cm^{-3}; and (b) 6.3×10^{12} and 6.5×10^{15} molecule cm^{-3}. The experiments were performed at $P = 75.5$ Torr

CHAPTER III

ÖH-ISOPRENE REACTION STUDIED USING LP/LIF

For the study of the pressure dependence for the reaction between OH and isoprene, the laser photolysis/laser induced fluorescence (LP/LIF) technique was applied. The pressure-dependent rate constants for the reaction of isoprene initiated by OH radical have been measured in the pressure range of 500 mTorr to 20 Torr. We obtained the low pressure limiting rate constant and high pressure limiting constant by fitting our data to the Troe expression.[16,88]

3-1. Experimental

The kinetic experiment was performed using a slow flow reactor with laser-photolysis /laser induced fluorescence(LP/LIF) detection.

Chamber

The experimental system used in this study consisted of a reactor, a Nd : YAG and dye laser and photomultiplier tube. The schematic diagram of this apparatus is given in Figure 8. The main chamber was made of stainless steel with perpendicular side arms, gas inlets and gas outlet to a high-throughput mechanical vacuum pump. The fused silica windows were used for the entrance and exit windows of the laser beam to excite the fluorescence at Brewsters's angle. Three different baratron gauges of 1, 10, and
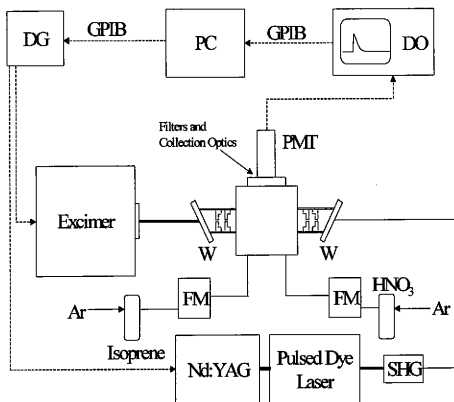
Figure 8. Schematic diagram of the experiment. DG = delay generator,
PC = personal computer, PMT = photomultiplier tube,
W = window placed at Brewster's angle, FM = flow meter,
SHG = second harmonic generator

1000 Torr full scales capacitance (MKS) were used. The baratron inlet was located about 25cm from the gas inlet. Isoprene (Aldrich, 99%) in the bubbler held at -15.0°C was delivered to the reactor using a flow controller (MKS model 1179A). A Welch 1402 mechanical pump was used to evacuate the reactor.

Laser

A Q-switched Nd: YAG laser (Spectra Physics GCR-150-10) with a pulse width of 8 ns full width at half maximum (FWHM) was used. A potassium dihydrogen phosphate (KD*P) crystal was used to frequency double the 1064 nm output of the Nd: YAG laser to 355nm. The power level at 355 nm was maximized by adjusting the orientation of the KD*P crystal. The BBO crystal was used to frequency double output of the dye laser (LAS, LDL 2051). The dye laser was pumped by the 355 nm second harmonic of a Q-switched Nd:YAG laser with a resolution of 0.07 cm^{-1} FWHM. Rhodamine 575 dyes (Exciton Inc.) was used in the dye laser. The final UV output had a resolution of ~0.14 cm^{-1} with a power of about 8 mJ/pulse and reduced 20μJ/pulse. A Molectron power meter measured the laser power. The dye laser was controlled by a PC. The scan mode was used to produce the LIF spectra of the hydroxyl radicals. The scan mode allowed the wavelength region scanned and the rate at which it was scanned to be varied. The manual mode allowed the laser to be set at a fixed wavelength, which could be changed manually.

OH Radical Generation

Photolysis and probe laser beams were counter-propagated through the windows in order to generate OH radicals and detect them. As a source of OH radicals concentrated nitric acid (HNO_3) was introduced into the chamber vertically to the laser beams, prepared by bubbling a ~ 5% mixture in argon carrier gas. OH radicals were generated by the photolysis of concentrated HNO_3 at 193 nm (ArF excimer laser). The photolysis of HNO_3 results either in OH plus NO_2 or in $O(^1D)$ plus HONO, with approximately equal yields.[89] In addition, the reactions of $O(^1D)$ with residual water vapor from HNO_3 also form OH radicals. Because $O(^1D)$ can affect the reaction of isoprene with OH, we evaluated the reaction of $O(^1D)$ using a computer model. The model included the collisional deactivation of $O(^1D)$ by water and isoprene, the reaction of $O(^1D)$ with water vapor and the hydrogen abstraction of $O(^1D)$ from isoprene.[16,90] The effects of the $O(^1D)$ were considered negligible after approximately 15 μs due to effective conversion of $O(^1D)$ to OH. The secondary reactions between isoprene and NO_2 or HONO from the photolysis of nitric acid were minor due to an excess of isoprene in the system.

We monitored the hydroxyl radical decay using laser-induced fluorescence. The LIF detects the hydroxyl radicals, excited in the (1, 0) vibrational band of the OH ($A^2\Sigma^+ \leftarrow X^2\Pi$) transition at 285.1 nm by using the BBO-doubled output of a pulsed dye laser(LAS) with Rhodamine 575 pumped at 355nm by a Nd:YAG laser (Spectra Physics GCR-150-10). For measuring the hydroxyl radical concentrations, a rotational line corresponding to the $Q_1(1)$ transitions was used. The fluorescence was collected

perpendicularly from the laser beam using two 25mm focusing lenses and detected using a photomultiplier tube (PMT). The PMT was a Hamamatsu model (Hamamatsu R374) with a UV grade silica casing. The PMT was sensitive from 200 – 900 nm with a gain of 10^6 and a rise time of 2 ns. In case of scattering light, BK7 filters that cut off the wavelength below 300 nm and visible filters were placed in front of the collection optics before the entrance slit of the PMT, which is a band pass filter effectively minimizing the scattering light from the photolysis and probe lasers. The fluorescence signals were averaged from 25 probe laser shots. A step size was taken between 0.25 and 1μs in over 100 time steps. The output signal (fluorescence) from the PMT was sent to a 400 MHz oscilloscope (Lecroy 9310A) and digitized. The timing between the laser pulses was controlled by a digital delay generator (Stanford Research DG535).

All experiments were performed under slow-flow condition in order to avoid the accumulation of photolysis or reaction products. We estimated the initial OH concentration of ~ $5x10^{10}$ molecules cm^{-3}. The lowest concentration of isoprene was about 3 orders of magnitude higher than that of OH radicals, which is under pseudo-first-order conditions.

To further validate our approach, we studied the rate constants for the reaction between OH and ethane using the similar approach. The reaction of C_2H_6 with hydroxyl radicals was performed at 298K and 10 Torr. Pure ethane (Aldrich, 99+% purity) was introduced and a 10 Torr capacitance manometer was used to estimate the concentration of ethane. The concentrations of ethane were 1×10^{15} to 1×10^{16} molecules cm^{-3}, which is under pseudo-first order approximation. The decay of OH signals was measured at 10 Torr total pressure, shown in Figure 9a. No pressure dependence of this reaction was

observed and the rate constant of $(2.5 \pm 0.2) \times 10^{-13}$ cm^3 molecules^{-1} s^{-1} was obtained as

shown in Figure 9b and agreed well with literature value.[16]

3-2. Results and Discussion

The kinetic studies for the reaction of isoprene initiated OH radicals were

investigated at pressure between 0.5 and 20 Torr and at room temperature. All kinetic

experiments were carried out under the pseudo-first order assumption, which is the

concentration of isoprene is around 2 order of magnitude higher that that of OH.

Thermalized OH Radical Preparation

The highly rotationally excited hydroxyl radical (OH) was formed from the

photolysis of HNO$_3$ and additional reaction of O(^{1}D) atoms with water in large rotational

temperatures.[91] The rotational relaxation of OH radicals was tested by LIF spectra of the

Q_1 and R_1 branches of the $1 \leftarrow 0$ band as a function of the delay time. Rotational

temperature was estimated by simulation of the spectra including available spectroscopic

information.[92] Since the rotational temperature was near 700 K at early time and

decreased significantly with delay time, a delay time offset >15 μs was used to get both

thermalized OH radicals and a negligible amount of O(^{1}D). Figure 10a represents a series

of typical pseudo-first order decays of the OH signal as a function of reaction time. A

linear least squares fit of the OH decays provides the pseudo-first order loss rate. The

slope of the logarithm of the OH signal as a function of reaction time corresponds to the

observed first-order rate coefficients (k^1). The initial concentration of OH was
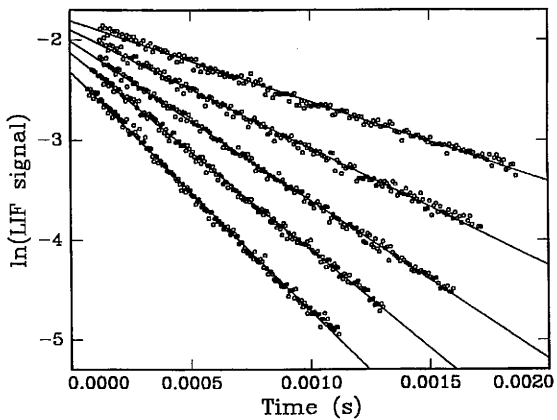
Figure 9a. Logarithm plot of the integrated fluorescence decay as a function of time at various concentrations of ethane. P = 10 Torr

Figure 9b. First-order loss rate coefficient k^I as a function of ethane concentration at 10 Torr

estimated ~5 x 10^{10} molecules cm^{-3} and isoprene concentrations were varied between 0 and 8.83 x 10^{14} molecules cm^{-3}. Secondary reactions are not expected to interfere because of no curvature in the OH decay plot which shows that the rotational distribution of the OH radical is thermalized and O(^{1}D) has a minor effect on the observed kinetics. Figure 10b shows the first-order coefficients as a function of isoprene concentrations. The slope of the linear least-square fit to the measured data provides an effective bimolecular rate constant for the reaction of isoprene with OH radicals. The rate constant of (1.00 ± 0.05) x 10^{-10} cm^3 molecules^{-1} s^{-1} was obtained at a pressure of 10 Torr. The rate constants at varied pressures are summarized in Table 4. In the pressure region of 500 mTorr to 20 Torr the rate constants vary from 7.31 x 10^{-11} to 1.03 x 10^{-10} cm^3 molecules^{-1} s^{-1}.

Table 4. Summary of pressure-dependence rate constants for the reaction of isoprene with OH at 295K determined by using LP/LIF

| Pressure (Torr)	K (cm^3 molecule^{-1}s^{-1})
20	(0.99 ± 0.05) x 10^{-10}
10	(1.00 ± 0.05) x 10^{-10}
1	(0.88 ± 0.06) x 10^{-10}
0.5	(0.76 ± 0.08) x 10^{-10}
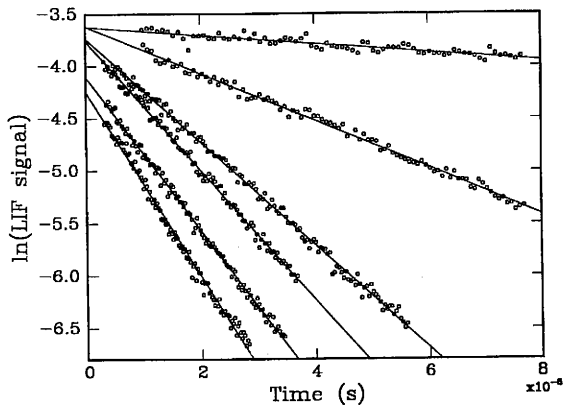
Figure 10a. Logarithm plot of the integrated fluorescence decay as a function of
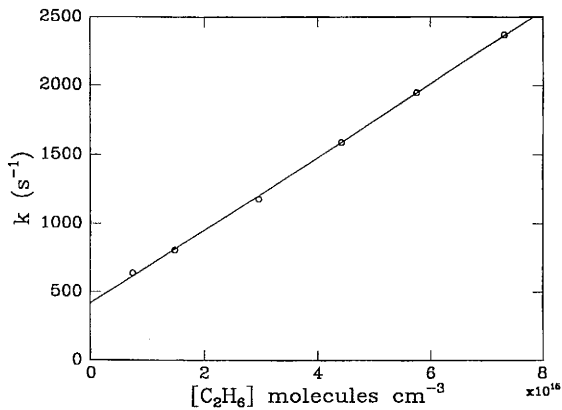time at various concentrations of isoprene, P = 10 Torr
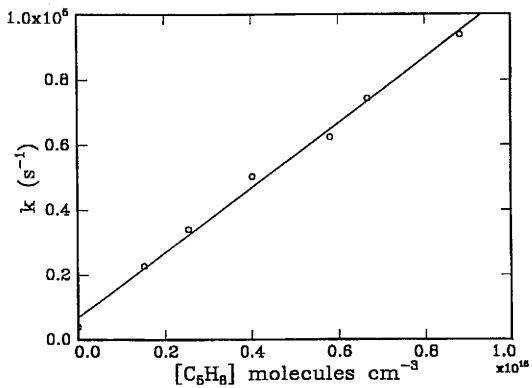
Figure 10b. First-order loss rate coefficient k^I as a function of isoprene concentration
at 10 Torr bimolecular rate constants as a function of pressure

<u>Falloff Regime</u>

In order to explain the fall off behavior of the OH addition reaction to isoprene, the pressure dependence rate constants can be described by the Troe expression [88]

$$k = \frac{k_0[M]}{(1 + k_1[M]/k_1)} 0.6^{\{1+(\log k_0[M]/k_1)^2\}^{-1}}$$

A least-squares iterative fit of the data to this expression yields a low pressure limiting termolecular rate constant (k_o) of $(6.98 \pm 2.2) \times 10^{-26}$ cm^6 molecules^{-2} s^{-1} and a high pressure limiting rate constant (k_1) of $(1.04 \pm 0.04) \times 10^{-10}$ cm^3 molecules^{-1} s^{-1} at 295 K as shown in Figure 11. This high-pressure limiting rate constant agrees with the recommended high-pressure rate constant.[40] The measured rate constant of (0.99 ± 0.05) $\times 10^{-10}$ cm^3 molecules^{-1} s^{-1} at 20 Torr seems to be near the beginning of the falloff regime. The rate constants decrease distinctively as the total pressure is reduced from 20 Torr to 500 mTorr. The data in Table 4 indicate the lowest pressures accessible in these experiments are at the low-pressure termolecular regime. However, a recently reported work by Stevens, et al.[39] on the OH-isoprene reaction using LIF detection of the OH radical in a flow reactor shows a significant difference from this study at the low-pressure termolecular regime. Their rate constant at 300 K in 2 Torr of He was $(1.10 \pm 0.05) \times 10^{-10}$ cm^3 molecules^{-1} s^{-1}, which is slightly higher than the recommended high-pressure rate constant.[40] In contrast, our study shows that a rate constant of $(0.88 \pm 0.05) \times 10^{-10}$ cm^3 molecules^{-1} s^{-1} at 295 K and in 1 Torr of Ar lies at the falloff regime. McGivern et al.[93] have evaluated the rate constant at 298 K in 2 Torr of He for the OH-isoprene reaction,

using RRKM/ME calculations to verify the difference between the use of argon and helium as buffer gases. The authors used the parameters from the CVTST calculations for the RRKM/ME calculations in 2 Torr of helium. Lennard-Jones parameters of $\varepsilon = 69.0$ K and $\sigma = 4.28$ Å were used to describe the He-adduct interaction.[94] The calculated rate constant at 298 K in 2 Torr of He is 0.86×10^{10} cm^3 molecules^{-1} s^{-1}, which is significantly lower than the rate constant in 2 Torr of He reported by Stevens et al.[39] However this calculated value is slightly smaller than the measured rate constant in 2 Torr of Ar in this work. The measured pressure dependent rate constants in the pressure range of 500 mTorr to 20 Torr provide the fall-off regime for the OH addition reaction to isoprene.
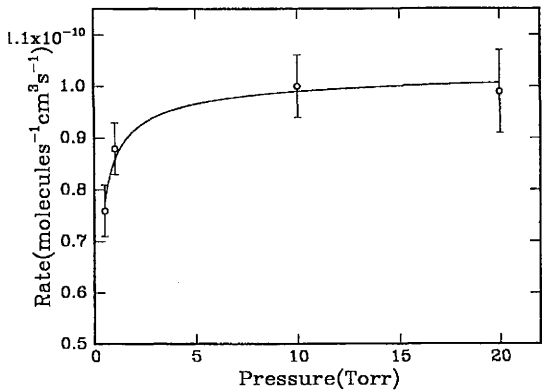
Figure 11. The pressure dependent rate constants were determined. The solid line represents a fit of the experimental data

CHAPTER IV

CL-ISOPRENE REACTION STUDIED USING CIMS

The work described in this chapter includes the study of the oxidation reactions of isoprene initiated by Cl atoms, using a fast-flow reactor coupled with chemical ionization mass spectrometry (CIMS). This reaction was studied both in the presence and absence of O_2 in order to explore the degradation pathways. The experimental measurements included the bimolecular rate constant and pressure dependence. We also identified the intermediates formed from the oxidation reactions of isoprene initiated by Cl. We directly observed the Cl-isoprene adduct in order to extract the rate constant of isoprene reactions by Cl atoms. A branching ratio for this reaction was obtained using HCl formation. The increase of the HCl signal intensity corresponded to the fraction of consumed concentration of Cl to form HCl when the varied isoprene was added. By monitoring the temporal evolution of the OH-isoprene adduct and Cl-isoprene adduct in the absence and presence of oxygen molecules, we also obtained the overall rate constants of the Cl-isoprene adduct in the presence of O_2.

4-1. Experimental

Reactor and Flow Conditions

The flow reactor used for the Cl-isoprene reaction was similar to that previous discussed to study the OH-isoprene reaction, with some modification. The flow reactor was made of precision-bore Pyrex tubing 1.78 cm in internal diameter and 60 in length. The inlet for isoprene is a series of five orifices (2 mm in diameter) located 5-cm apart at

the downstream end of the flow tube. The hole was enclosed in a Pyrex sleeve, which was sealed to the reactor tube. The flow of the reactants was controlled by glass vacuum valves with Teflon plugs. The reactant addition orifices were designed to minimize disturbance of the viscous flow. All inner surfaces of the flow reactor exposed to Cl were coated with a halocarbon wax to reduce the wall loss of Cl atoms. Helium carrier gas in the range of 1 to 3 STP l min^{-1} was flowed into the flow reactor through an entrance port in the rear of the flow reactor. Typical flow velocity in the flow reactor ranged from 1300 to 2500 cm s^{-1}. The pressure in the flow reactor was regulated between 5 and 10 Torr and all experiments were performed at 298 ± 2 K.

As described above, the distance for fully developed laminar flow can be estimated according to the expression of $l = 0.115aRe$.[74] Our experimental conditions had a typical value of 25 for the Reynolds number. The length for the fully developed laminar flow was determined to be about 3 cm, which is significantly less than that of the flow reactor. The pressure-independent gas-phase diffusion coefficients, pD, of isoprene and Cl were 365 and 602 Torr cm^2 s^{-1}, respectively. Thus Cl and isoprene were homogeneously mixed in our experiments.

Cl Atom Preparation

Two different methods were used to *in situ* generate the chlorine atoms. One way is that Cl atoms were introduced into the flow reactor by passing a small flow of (0.1 – 1)% Cl_2 / He mixture through a microwave discharge. Another way is that a (0.1 – 1)% H_2 / He mixture flowed through the microwave discharge and then reacted with an excess of Cl_2 downstream,

$$H + Cl_2 \rightarrow HCl + Cl \qquad (12)$$

The kinetic results obtained from those techniques were similar within the uncertainty of our present experiments. We proceeded with the former method in the majority of the experiments in this study. Cl was detected in the negative ion mode using SF_6^- as the reagent ions, following by the ion-molecule reaction,

$$Cl + SF_6^- \rightarrow Cl^- + SF_6 \qquad (13)$$

The ion-molecule reaction rate constant for reaction (13) has not been measured yet. The Cl concentration was determined using the bromine titration method,

$$Cl + Br_2 \rightarrow BrCl + Br \qquad (14)$$

with an excess of Br_2. The bimolecular rate constant for this reaction is 2.3 x 10^{-10} exp{-(135 $\pm$ 60)}/T) cm^3 molecule^{-1} s^{-1}.[71] The concentration of Cl atoms was calculated by [Cl] = Δ[Br_2] = [BrCl]. Alternatively, we also inferred the chlorine atom concentration from the measurement of dissociated fraction of chlorine molecules introduced to the flow reactor, according to [Cl] $\approx$ 2Δ[Cl_2]. Δ[Cl_2] is the difference in the chlorine concentrations when the microwave discharge was switched off and on. The flow through a quartz cell used in the Evenson cavity was coated with a concentrated phosphoric acid to enhance the dissociation efficiency of the chlorine molecules. Typically the concentration of chlorine atoms in the flow reactor was estimated in the range of (1 to 5) x 10^9 molecule cm^{-3}.

4-2. Results and Discussion

Isoprene Reaction with Cl

The reaction between Cl and isoprene proceeds through two channels. The major channel is Cl addition to isoprene resulted in Cl-isoprene adduct formation and the minor is hydrogen abstraction to form HCl.

$$Cl + C_5H_8 \rightarrow C_5H_8Cl \qquad (15a)$$

$$Cl + C_5H_8 \rightarrow C_5H_7 + HCl \qquad (15b)$$
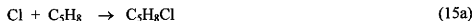
The kinetic studies of the reaction of isoprene initiated by chlorine atoms were investigated under the pseudo-first order approximation, using isoprene as the excess reagent. The observed first order loss rate coefficients (k^I, s^{-1}) were derived directly based on the plot of the decay of the Cl atoms signal as a function of the reaction distance. The bimolecular rate constants were obtained by the fitting of the plot of k^I vs. the concentration of isoprene.

Figure 12a presents the pseudo-first order decay of Cl in the presence of isoprene. The slope of the plots of the logarithm of Cl signal vs. reaction time represents the observed first-order rate coefficients (k^I). The secondary reactions in our experiments were negligible since those plots were linear. The experimental conditions were at P = 8.7 Torr and Re = 23. The initial concentration of Cl was estimated as 3.0×10^9 molecule cm^{-3} and the isoprene concentrations were varied between 4.6×10^{10} and 1.5×10^{11} molecule cm^{-3}. The background signals of Cl (35 m/e) produced in the system were subtracted from all the points.

The effects of axial and radial diffusion of the reactants were estimated by the Brown approach. The pressure-independent diffusion coefficients for Cl in helium, D_{Cl-He}

was 508.76 torr cm^2 s^{-1} at P = 8 Torr and T = 298 K. The correction due to gas-phase diffusion in the axial and radial directions was less than 3 %. The bimolecular rate constant was obtained directly from the observed first-order loss coefficient for Cl because this correction was smaller than the random and systematic errors estimated in our experiments. Figure 12b shows the first-order coefficient as a function of isoprene concentration. The slope of the linear least squares fit to the experimental data provides an effective bimolecular rate constant for the reaction of isoprene with Cl atoms with a value of 4.1 x 10^{-10} cm^3 molecule^{-1} s^{-1}. Note that in Figure 12a the Cl concentration was reduced to approximately 30 % of it's original value at the highest isoprene concentration. Due to the existence of the background signal at m/e = 35 (about 10 to 15 % of the original signal), we did not further increase the final Cl removal.

We performed similar experiments in the pressure range of 5 to 10 Torr, with measured rate constants of (3.8 ± 0.4), (4.1 ± 0.2), (4.0 ± 0.2), and (4.1 ± 0.3) x 10^{-10} cm^3 molecule^{-1} s^{-1} at 6.6, 8.2, 8.7, and 9.2 Torr, respectively. Each of the data represents at least four individual measurements at various initial concentration of isoprene and Cl. The average rate constant over the pressure range of 5 to 10 Torr is (4.0 ± 0.3) x 10^{-10} cm^3 molecule^{-1} s^{-1}, where the quoted uncertainty represents the scatter in the data in one sigma deviation without including systematic errors. The systematic uncertainty in our measured rate constants was estimated within ± 10%, with sources of error in the measurement such as gas flows, temperature, detection signal, and pressure and in the flow considerations.
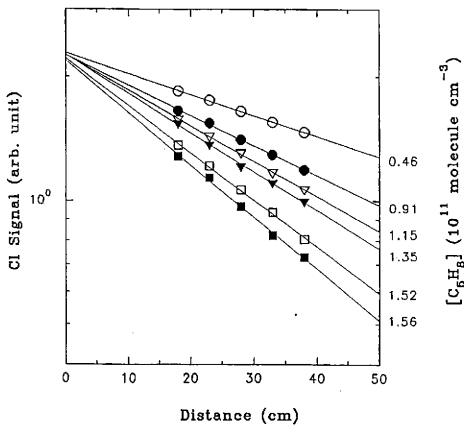
Figure 12a. Decay of Cl signal as a function of injector distance at various concentrations of isoprene. Experimental conditions are: P = 8.7 Torr, U = 2301, and *Re* = 23
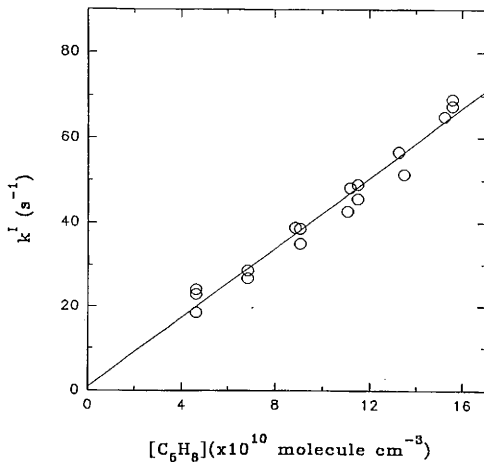
Figure 12b. First-order loss rate coefficient k^I as a function of isoprene concentration. Experimental conditions are similar to those in Figure 12a

Our measured rate constant between isoprene and Cl in the pressure range of 5 to 10 Torr is generally in good agreement with the results presently available in the literature.[67-71] The summary of the previous measurements of the rate constants near room temperature is shown in Figure 13. Ragains and Finlayson-Pitts[67] measured a rate constant of $(4.0 \pm 0.4) \times 10^{-10}$ cm^3 molecule^{-1} s^{-1} at 5 Torr, in excellent agreement with the results reported in this study. Our value is slightly higher than those reported by Notario et al.[70] and Bedjanian et al.[71], whose measured rates are $(3.6 \pm 0.4) \times 10^{-10}$ cm^3 molecule^{-1} s^{-1} in the pressure range of 15 to 60 Torr and $(3.4 \pm 0.5) \times 10^{-10}$ cm^3 molecule^{-1} s^{-1} in the pressure range of 0.25 to 3.0 Torr, respectively. The difference between our measured rate and those two latter studies, however, is within the quoted uncertainties of the respective work. Our results are also in good agreement with those recently measured by Canosa-Mas et al[69] whose measured values are $(4.0 \pm 0.8) \times 10^{-10}$ cm^3 molecule^{-1} s^{-1} at 760 Torr. Note that the largest disagreement for the reaction between Cl and isoprene among the various studies occurs at 760 Torr. For example, the values reported by Fantechi et al.[68] is about 40 % higher than that recently reported by Canosa-Mas et al.[69]. Our measured rate constant in the pressure range of 5 to 10 Torr is very close to the value reported by Canosa-Mas et al.[69] at 760 Torr.

Figure 13. Bimolecular rate constant for the reaction of isoprene with Cl as a function of pressure. The different symbols are measurements reported by different in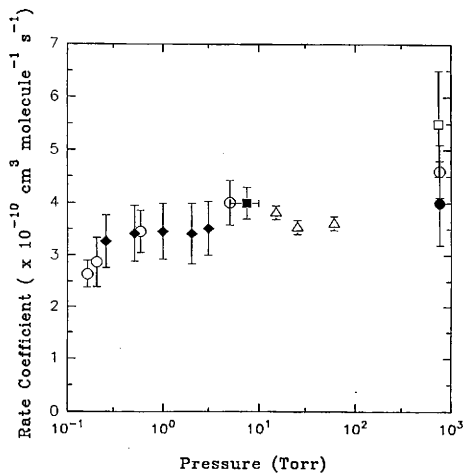vestigators: solid square (this work), open circles (ref. 67), open square (ref.68), solid down-triangles (ref. 69), open up-triangles (ref. 70), and solid diamonds (ref. 71)

Branching Ratio

In order to obtain the branching ratio for reaction (15) we performed experiments to study the HCl formation. This approach is described well by Bedjanian et al.[71] Cl atoms were generated through microwave discharge of Cl_2 with a carrier gas of He. With an excess of isoprene, we monitored the decrease of the signal intensity of Cl with the increase of the signal intensity of HCl formed. The concentrations of isoprene were varied between 3.0×10^{11} and 1.3×10^{11} molecule cm^{-3}. The signals of HCl (55 m/e) formed were measured as F•HCl by using negative reagent ions, SF_6^-. The increase of HCl signal intensity (Δ[HCl]) corresponded to the fraction of consumed Cl concentration, (Δ[Cl]), as the concentrations of isoprene were varied. The plot of the increase of HCl signals as a function of Δ[Cl] yields the branching-fraction of the product for reaction (15). In Figure 14, the slope of the fitted line yields k_{1b}/k_1 with a value of (17.4 ± 0.4)%, where the uncertainty stands for 2σ standard deviation with an addition of 5% systematic error. The branching ration we obtained is in excellent agreement with those measured in previous studies.[67,71]

The Observation of the Cl-Isoprene Adduct

We monitored the formation of the Cl-isoprene adduct using the CIMS method. Bedjanian et al.[71] has reported the detection of the Cl-isoprene adduct, using electron impact (EI). This approach, however, results in a significant fragmentation for this adduct, because EI applied energetic electron of the ionization, prohibiting kinetic
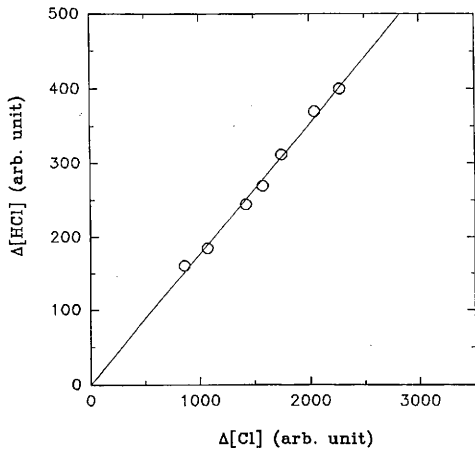
Figure 14. Formation of HCl from the reaction of Cl with isoprene. The reaction
distance was increased by 20 cm at about 42 s and was returned to the
initial distance at about 80 s

information to be derived. In order to detect the Cl-isoprene adduct we used O_2^+ reagent ions according to the ion-molecule reaction,

$$O_2^+ + C_5H_8Cl \rightarrow C_5H_8Cl^+ + O_2 \qquad (16)$$

The rate constant of the above ion-molecule reaction has not been measured yet. According to the previous mechanistic studies, the reaction (15) may result in four different isomeric radicals in Figure 15. *Ab initio* calculation indicate that Cl addition to the C1- and C4- positions are the most energetically favorable channels with about 14 kcal mole $^{-1}$ less than to the C2- and C3- positions. Because the CIMS is incapable of discriminating isomers, we refer to the product as the "Cl-isoprene adduct" with 103 m/e of C_5H_8Cl. The isomeric effect on the overall rate constants would be negligible in our study.

We took several procedures to verify that the signal of 103 m/e is indeed *from* the Cl-isoprene adduct, not from secondary ion-molecule reactions. First, we monitored the disappearance of the signal at 103 m/e when the reactants ceased to be introduced into the reactor. The adduct signal was observed to increase when the reaction time was increased. Figure 16 (a) and (b) show an example of Cl-isoprene formation in accordance with the decay of Cl atoms. The experimental conditions were: P=9.2 Torr, Re = 15, U = 1341 cm s^{-1}, and $[C_5H_8]$ = 7.5 x 10^{11} molecule cm^{-3}. An effective bimolecular rate constant was obtained from the disappearance of Cl signals in 16(a) with a value of 4.1 x 10^{-10} cm^3 molecule^{-1} s^{-1}. As shown in this figure, there is a gradual

increase in the Cl-isoprene adduct signal when the reaction distance increased. In Figure 16(b), a numerical simulation was used to derive a rate coefficient for the reaction of isoprene with Cl. The computer model included the initial concentration of Cl, isoprene, and all other precursors. Using the measured branching ratio based on HCl formation to constrain the fitting, the rate constant for reaction 15(a) was varied to fit the observed Cl-isoprene adduct formation profile. The solid line in Figure 16(b) represents the best fit to the observed formation of the Cl-isoprene adduct, with a value of 3.4×10^{-10} cm^3 molecule^{-1} s^{-1}. Note that the results shown in Figure 16 were performed in separate runs between the decay of Cl atoms and the formation of Cl-isoprene adduct, using either negative or positive reagent ions, respectively. We estimated an uncertainty of 10 % associated with fitting the Cl-isoprene adduct formation. On the basis of the product studies, we also concluded that the secondary reactions of the Cl-isoprene adduct were not important in our experimental system and that heterogeneous loss of this adduct on the surfaces of the flow reactor appeared to be minimal in our experiments. This approach is similar to the investigation of OH-isoprene adduct as mentioned in Chapter II.

Cl-Isoprene Adduct Reaction with O$_2$

Reaction (17) has been studied by monitoring the temporal profiles of the Cl-isoprene adduct in the presence of oxygen molecules, O$_2$,

$$C_5H_8Cl \; + \; O_2 \rightarrow C_5H_8ClO_2 \qquad (17)$$

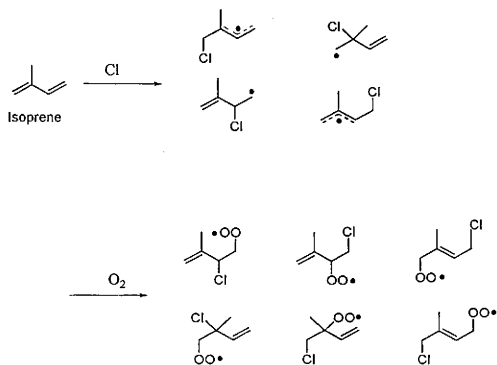Figure 15. A mechanistic diagram for the reactions of Cl with isoprene and the Cl-isoprene adduct with O_2
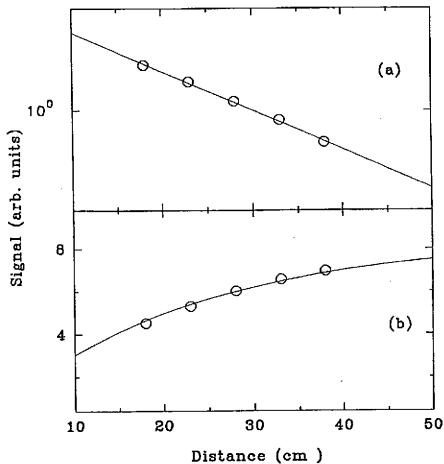
Figure 16. Variation of the Cl(a) and Cl-isoprene adduct(b) signals as a function of
reaction time. The solid curves are from model calculations (see text).
Experimental conditions are: P = 9.6 Torr, U = 1424 cm s^{-1}, Re = 15, and
[C$_5$H$_8$]$_o$ = 2.8 x 10^{11} molecule cm^{-3}

The procedures to derive a rate constant between the Cl-isoprene adduct and O_2 involved two steps. First, we measured the signals at mass 103 corresponding to the Cl-isoprene adduct, as the reaction time increased in an absence of O_2. Then we repeated the same experiment in the presence of oxygen molecules. As described above, fitting the experimental data using the simulation varied the bimolecular rate constant for the formation of the Cl-isoprene adduct in the absence of O_2. The computer model then included this rate constant in addition to the reaction of the Cl-isoprene adduct with O_2. The reaction rate between the Cl-isoprene adduct and O_2 was then determined by best fitting the observed adduct data. In the presence O_2, the reaction rate constants used in our computer modeling are represented in Table 5. The relevant kinetic information was obtained from the JPL publication.[16]

The temporal evolution of the Cl-isoprene adducts in the presence and absence of O_2 was presented in Figure 17(a). The production of the Cl-isoprene adduct is diminished in the presence of O_2, which is due to the formation of the peroxy radicals from the reaction between the Cl-isoprene adduct and O_2. The initial concentration of isoprene and O_2 were 1.4×10^{11} and 2.7×10^{15} molecule cm^{-3}, respectively. Figure 17(a) shows the bimolecular rate constant of the reaction between isoprene and Cl atoms in terms of the formation of the Cl-isoprene adduct by fitting the data with a value of 4.0×10^{-10} cm^3 molecule^{-1} s^{-1}. The best fit to the Cl-isoprene adduct in the presence of O_2 in Figure 17(b)

gives a rate constant for the reaction of the Cl-isoprene adduct with O_2, yielding a value of 1.0×10^{-14} cm^3 $molecule^{-1}$ s^{-1}. Figure 18 depicts the production of the Cl-isoprene adduct as a function of O_2 concentration in the range of 0 to 8.9×10^{15} molecule cm^{-3}. The initial concentration of isoprene was 2.7×10^{11} molecule cm^{-3}. As is seen in this figure, a lesser production of the Cl-isoprene adduct at a higher concentration of oxygen molecules is due to the reaction between the Cl-isoprene adduct and O_2. The best fit to the data yields the rate constant of 1.0×10^{-14} cm^3 $molecule^{-1}$ s^{-1}. We performed the several experiments, applying different pressures, initial concentrations of isoprene and O_2 conditions. The average rate constant for the reaction of the Cl-isoprene adduct with O_2 was $(1.0 \pm 0.3) \times 10^{-14}$ cm^3 $molecule^{-1}$ s^{-1} in the pressure range of 5 to 10 Torr, where the quoted uncertainty indicates the scatter in the data at the one standard deviation level. We estimated about $\pm$ 50 % systematic error in the present data, which are from the uncertainties of modeling of the Cl-isoprene adduct and experimental measurements of gas flows, temperature and pressure.

Table 5. Summary of the chemical reactions used in computer simulations for the system involving Cl, isoprene, and O_2

Reaction	k^a (cm^3 molecule^{-1} s^{-1})
$C_5H_8 + Cl \rightarrow C_5H_7 + HCl$	6.6×10^{-11} [b]
$\rightarrow C_5H_8Cl$	3.4×10^{-11} [b]
$C_5H_8Cl + O_2 \rightarrow C_5H_8ClO_2$	1.0×10^{-14} [b]
$Cl + O_2 \rightarrow ClO_2$	7.7×10^{-16}
$Cl + OClO \rightarrow ClO + ClO$	5.8×10^{-11}
$Cl + ClO_2 \rightarrow Cl_2 + O_2$	2.3×10^{-10}
$\rightarrow ClO + ClO$	1.2×10^{-11}
$ClO + ClO \rightarrow Cl_2O_2$	6.1×10^{-15}
$ClO + ClO \rightarrow Cl_2 + O_2$	4.8×10^{-15}
$\rightarrow ClOO + Cl$	8.0×10^{-15}
$\rightarrow OclO + Cl$	3.5×10^{-15}
$ClO + OClO \rightarrow Cl_2O_3$	1.8×10^{-14}
$Cl + Cl_2O_2 \rightarrow$ Products	1.0×10^{-10}

[a] Rate constants are from ref 16 at 298 K and 9 Torr, except noted otherwise.
[b] From this work.
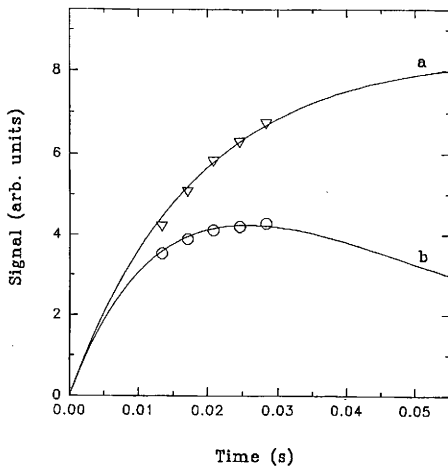
Figure 17. Production of the Cl-isoprene adduct as a function of the reaction time in the absence (triangles) and presence (squares) of O_2. The solid curves are from model calculations(see text). $[C_5H_8]_0 = 1.4 \times 10^{11}$ molecule cm^{-3}, $[O_2]_0 = 2.7 \times 10^{15}$ molecule cm^{-3} in (b). The experimental conditions are: P = 9.2 Torr, U = 1341 cm s^{-1}, and $Re = 15$
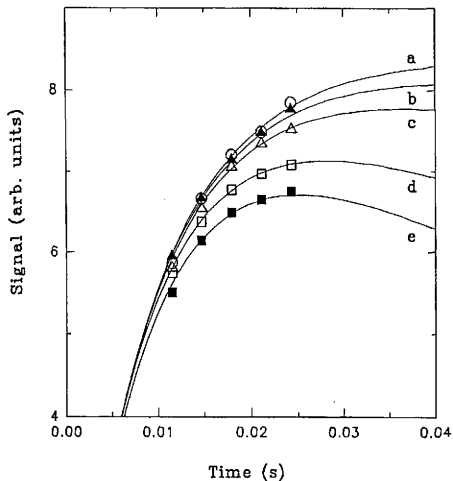
Figure 18. Production of the Cl-isoprene adduct as a function of the reaction time at various O_2 concentrations (x 10^{15} molecule cm^{-3}): (a) 0 (open circles), (b) 0.9 (solid down triangles), (c) 2.1 (open up-triangles), (d) 5.8 (open squares), and (e) 8.9 (solid squares). The solid curves are from model calculations (see text). $[C_5H_8]_0 = 2.7$ x 10^{11} molecule cm^{-3}. The experiments were performed at P = 8.2 Torr, U = 1563 cm s^{-1}, and Re = 14

CHAPTER V

CONCLUSIONS

We have presented kinetic studies of isoprene reactions initiated by the OH radical and the Cl atom, using a fast flow reactor/chemical ionization mass spectrometry (CIMS) and laser photolysis/laser induced fluorescence (LP/LIF) detection. The rate constants for the OH-isoprene reaction using the CIMS approach were measured at a pressure range of 70 to 112 Torr with a value of $(9.7 \pm 1.0) \times 10^{-11}$ to $(10.5 \pm 1.1) \times 10^{-11}$ cm^3 molecule^{-1} s^{-1} at 298 ± 2 K. The LP/LIF method was used to obtain the rate constants in the pressure range of 0.5 to 20 Torr, which shows a fall-off regime for the OH addition to isoprene, with a low pressure limiting termolecular rate constant $k_o =$ of 7.5×10^{-26} cm^6 molecules^{-2} s^{-1} and a high pressure limiting rate constant $k_1 =$ of 1.07×10^{-10} cm^3 molecules^{-1} s^{-1} at 295 K. The rate constant at 0.5 Torr is $(7.6 \pm 0.8) \times 10^{-11}$ cm^3 molecule^{-1} s^{-1}. The CIMS approach also allowed us to monitor the temporal profile of the OH-isoprene adducts. The observed bimolecular rate constant for the reaction between the OH-isoprene adduct and O_2 was determined to be $(2.8 \pm 0.7) \times 10^{-15}$ cm^3 molecule^{-1} s^{-1} at 75.5 Torr. The atmospheric lifetime of the OH-isoprene adduct can be estimated from the reaction rate constants measured in this study giving a value of approximately 3×10^{-4} s. This implies that the O_2 addition to the OH-isoprene adduct is the major reaction channel in the atmosphere.

For the reaction of isoprene with Cl atoms the CIMS method was employed, yielding a pressure independent rate constant of $(4.0 \pm 0.3) \times 10^{-10}$ cm^3 molecule^{-1} s^{-1} at pressure range of 5 to 10 Torr. The branching ratio for this reaction was also studied

based on HCl formation, giving a value of $(17.7 \pm 3.2)\%$. In addition, we obtained the first experimental overall rate constant for the reaction between the Cl-isoprene adduct and O_2 with a value of $(1.0 \pm 0.3) \times 10^{-14}$ cm^3 molecule^{-1} s^{-1}. The tropospheric lifetime of Cl-isoprene adduct with respect to addition reaction with O_2 can be estimated from the measured rate constants. This lifetime of approximately 2×10^{-5} s was calculated using the rate constant for the reaction between the Cl-isoprene adduct and O_2 and assuming an average atmospheric concentration of O_2 molecules at STP.

Hence in this work we have developed experimental techniques for the isoprene oxidation reactions with the OH radicals and Cl atoms, which should provide insight for understanding of the photochemical oxidation of isoprene in the atmosphere.

REFERENCES

(1) Guenther, A.; Hewitt, C.N.; Erickson, D.; Fall, R.; Geron, C.; Pierce, T.; Scholes, B.; Steinbrecher, R.; Tallamraju, R.; Taylor, J.; Zimmermann, P. *J. Geophys. Res.* **1995**, *100*, 8873.

(2) Guenther, A.; Geron, C.; Pierce, T.; Lamb, B.; Harley, P.; Fall, R. *Atmos. Environ.* **2000**, *34*, 2205.

(3) König, G.; Brunda, M.; Puxbaum, H.; Hewitt, C.N.; Duckham, S.C.; Rudolph, J. *Atmos. Environ.* **1995**. *29*, 861.

(4) Arey. J.; Corchnoy, S.B.; Atkinson, R. *Atmos. Environ.* **1991**, *25A*, 1377.

(5) Akinson, R. *J. Phys. Chem. Ref. Data Monogr.* **1994**, *2*, I.

(6) Seinfeld, J.H.; Pandis, S.N. *Atmospheric Chemistry and Physics: From Air Pollution to Climate Change*; John Wiley & Sons, Inc.: New York, 1997.

(7) National Research Council, *Rethinking the Ozone Problem in Urban and Regional Air Pollution.* National Academy Press: Washington, DC, 1991

(8) Logan, J. A. *J. Geophys. Res.* **1985**,*90*, 10482.

(9) Schwartz, S.E. *Science*, **1989**, *243*, 753.

(10) IPCC Scientific Assessment, *Climate Change*; Cambridge University Press: Oxford, 1992.

(11) World Meteorological Organization, "Scientific assessment of ozone depletion,": World Meteorological Organization Global Ozone Research and Monitoring Project - Report No. 37, Geneva, Switzerland, 1995

(12) Rasmussen, R.A.; Khalil, M.A. *J. Geophys. Res.* **1988**, *93*, 1417.

(13) Placet, M.; Battye, R.E.; Fehsenfeld, F.C.; Bassett, G.W. In *NAPAP SOST* Rep. 1: Natl. Acid Precipitation Assessment Program, Washington DC, 1990.

(14) Trainer, M. *Nature* **1987**, *329*, 705.

(15) Roelofs, G.J.; Lelieveld, J. *Tellus B*, **1997**, *49*, 38.

(16) DeMore, W.B.; Sander, S.P; Golden, D.M.; Hampson, R.F.; Kurylo, M.J.; Howard, C.J.; Ravishankara, A.R.; Kolb, C.E.; Molina, M.J., *Chemical Kinetics and Photochemical Data for Use in Stratospheric Modeling, Evaluation* No. 12 NASA

Panel for Data Evalution, Jet Propulsion Laboratory Publication , Pasadena, CA, January 15, 1997.

(17) Atkinson, R., *Int. J. Chem. Kinet.*, **1997**, *29*, 99.

(18) Paulson, S.E.; Orlando, J.J. *Geophys. Res. Lett.*, **1996**, *23*, 3727.

(19) Lloyd, A.C.; Atkinson, R.; Lurmann, F.W.; Nitta, B., *Atmos. Environ.* **1983**, *17*, 1931.

(20) Grey, M.W.; Whitten, G.Z.; Killus, J.P. "Development and Testing of the CBM-IV for Urban and Regional Modeling", EPA-600/3-88-012,1988

(21) Grey, M.W.; Whitten. J.P; Killus, J.P.; Dodge, M.C. *J. Geophys. Res.* **1989**, *94*,12925.

(22) Stockwell, W.R.; Middleton, P.; Chang, L.S.; Tang, X. *J. Geophys. Res.* **1990**, *95*, 16343.

(23) Carter, W.P.L. *Atmos. Environ.* **1990**, *23A*, 481.

(24) Akinson, R. *J. Phys. Chem. Ref. Data* **1997**, *26*, 251.

(25) Paulson, S.E; Seinfeld, J.H. *Int. J. Chem. Kinet.*, **1992**, *24*, 79.

(26) Carter, W.P.L. *Atmos. Environ.* **1996**, *30*, 4275.

(27) Lloyd, A.C.; Atkinson, R.; Lurmann, F.W.; Nitta, B. *Atmos. Environ.* **1983**, *17*, 1931.

(28) Killus, J.P.; Whitten, G.Z. *Environ. Sci. Tech.* **1984**, *18*, 142.

(29) Gu, C.I.; Rynard, C.M.; Hendry, D.G.; Mill, T. *Environ. Sci. Tech.* **1985**, *19*, 151.

(30) Atkinson, R; Aschmann, S.M.; Touazon, E.C.; Arey, J.; Zielinska, B. *Int. J. Chem. Kinet.* **1989**, *21*, 593.

(31) Tuazon, E.C.; Atkinson, R.. *Int. J. Chem. Kinet.* **1990**, *22*, 1221.

(32) Grosjean, D. *Environ. Sci. Tech.* **1993**, *27*, 830.

(33) Kwok, E.S.; Atkinson, R.; Arey, J. *Environ. Sci. Tech.* **1995**, *29*, 2467.

(34) Cox, R.A.; Derwent, R.G.; Williams, M.R. *Environ. Sci. Tech.* **1980**, *14*, 57.

(35) Atkinson, R; Aschmann, S.M.; Winer, A.M.; Pitts, J.N., Jr. *Int. J. Chem. Kinet.* **1982**, *14*, 507.

(36) Ohta, T. *J. Phys. Chem.* **1983**, *87*, 1209.

(37) Kleindlenst, T.E.; Harris, G.W.; Pitts, Jr., J.N. *Environ. Sci. Tech.* **1982**, *16*, 844.

(38) Siese, M.; Koch, R.; Fittschen, C; Zetzsch, In *Proceedings of Eurotrac Symposium '94; ed.* Borrel P.M. et al.; Academic Publishing: The Hague, 1994.

(39) Stevens, P.; L'Esperance, D.; Chuong, B.; Martin, G. *Int. J. Chem. Kinet.* **1999**, *31*, 637.

(40) Atkinson, R. *Int. J. Chem. Kinet.* **1996**, *28*, 731.

(41) Jenkin, M.E.; Boyd, A.A.; Lesclaux, R. *J. Atmos. Chem.* **1998**, *29*, 267.

(42) Arnts, R. R.; Gay, B.W. Jr. In *Photochemistry of Some Naturally Emitted Hydrocarbons*; EPA-600/3-79-081, 1979.

(43) Paulson, S.E.; Seinfeld, J.H. *J. Geophys. Res.* **1992**, *97*, 20703.

(44) Platt, U. In *European Commission,* Larson, B.; Versino, B.; Angeletti, G., Eds., Academic Publishing: The Hague, 1997

(45) DeHaan, D. O.; Brauers, T.; Oum, K.; Stutz, J.; Nordmeyer, T.; Finlayson-Pitts, B. J., *Inv. Rev. Phys. Chem.* **1999**, in press

(46) Graedel, T. E.; Keene, W. C., *Global Biogeochem. Cycl.* **1995**, *9*, 47.

(47) Keene, W. C. In *Naturally Produced Organohalogens,* Grimvall, A.; de Leer, E. W. B.; Eds.; Kluwer Academic Publisher, 1995, 363.

(48) Keene, W. C.; Jacob, D. J.; Fan, S. M., *Atmos. Environ.* **1996**, *30*, R1.

(49) Jabson, B. T.; Niki, H.M. Yokouchi, Y.; Bottenheim, J.; Hopper, F.; Leaitch, R. *J. Geophys. Res.* **1994**, *99*, 25355.

(50) Solberg, S.; Schmidbauer, N.; Semb, A.; Stordal, F.; Hov, O. *J. Atmos. Chem.* **1996**, *23*, 301.

(51) Wingenter, O. W.; Kubo, M. K.; Blake, N. J.; Smith, T. W.; Rowland , F. S. *J. Geophys, Res,* **1996**, *101*, 4331.

(52) Singh, H. B.; Thakur, A. N.; Chen, Y. E.; Kanakidou, M. *Geophys. Res. Lett.* **1996**, *23*, 1529.

(53) Rudolph, J.; Koppmann, R.; Plass-Dülmer, C. H. *Atmos. Environ.* **1996**, *30*, 1887.

(54) Graedel, T. E.; Keene, W. C. *J. Geophys. Res.* **1999**, *104*, 8331.

(55) Singh, H. B.,(ed.), *Chemistry and Climate of the Atmosphere*, Van Nostrand Reinhold, New York, **1995**.

(56) Pszenny, A. A. P.; Keen, W.,C.; Jacob, D. J.; Fan, S.; Maben, J. R.; Zetwo, M. P.; Springer-Young, M.; Galloway, J. N. *Geophys. Res. Lett.* **1993**, *20*, 699.

(57) Spicer, C. W.; Chapman, E. G.; Pinalyson-Pitts, B. J.; Plastridge, R. A.; Hubbe, J. M.; Fast, J. D.; Berkowitz, C. M. *Nature*, **1998**, *394*, 353.

(58) Keene, W. C.; Pszenny, A. A. P.; Jacob, D. J.; Duce, R. A.; Galloway, J. N.; Schultz-Tokos, J. J.; Sievering, H.; Boatman, J. F. *Global Biogeochem. Cycl.* **1990**, *4*, 407.

(59) Singh, H. B.; Kasting, J. F. *J. Atmos. Chem.* **1988**, *7*, 261.

(60) Wingenter, O. W.; Kubo, M. K.; Blake, N.J.; Smith Jr. T. W., Blake; D.R, Rowland; F. S. *J. Geophys. Res.* **1996**; *101*, 4331.

(61) Brauers, T.; Aschmutat, U.; Brandenburger, U.; Dorn, H. --P.; Hausmann, M.; Hessling, M.; Hofzumahaus, A.; Holland, F.; Plass-Dülmer, C.; Ehhalt, D. H. *Geophys. Res. Lett.* **1996**, *23*, 2545.

(62) Bonsang, B.; Polle, C.; Lambert, G. *Geophys. Res. Lett.* **1992**, *19*, 1129.

(63) Moore, R. M.; Oram, D. E.; Penkett, S. A. *Geophys. Res. Lett.* **1994**, *21*, 2507.

(64) Milne, P. J.; Reimer, D. D.; Zika, R. G.; Brand, L.E. *Marine Chem.* **1995**, *48*, 237.

(65) McKay, W. A.; Turmer, M.F.; Jones, B. M.R.M.; Halliwell, C. M. *Atmos. Environ.* **1996**, *30*, 2583.

(66) Ratte, M.; Bujok, O.; Spitzy, A.; Rudolph, J. *J. Geophys. Res.* **1998**, *103*, 5707.

(67) Ragins, M. L.; Finlayson-Pitts, B. J. *J. Phys. Chem.* **1997**, *101*, 1509.

(68) Fantechi, G.; Jensen, N. R.; Saastad, O.; Hjorth, J.; Peeters, J. *J. Atmos. Chem.* **1998**, *31*, 247.

(69) Canosa-Mas, C. E.; Hutton-Squire, H. R.; King, M. D.; Stewart, D. J.; Thompson, K. C.; Wayne, R. P. *J. Atmos. Chem.* **1999**, *34*, 163.

(70) Notario, A.; Le Bras, G.; Mellouki, A. *Chem. Phys. Lett.* **1997**, *281*, 421.

(71) Bedjanian, Y.; Laverdet, G.; Le Bras, G. *J. Phys. Chem.* **1998**, *102*, 953.

(72) Seeley, J.V.; Jayne, J.T.; Molina, M.J. *Int. J. Chem. Kinet.* **1993**, *25*, 571.

(73) Kundsen, J. G.; Katz, D. L. *Fluid Dynamics*, McGraw-Hill: New York, 1958.

(74) Langhaar, H. L. *Am. Soc. Mech. Eng. Trans.* **1942**, *64*, A55.

(75) Taylor, G. *Proc. R. Soc. London, Ser. A.* **1953**, *219*, 186.

(76) Zhang, R.; Molina, L.T.; Molina, M.J. *Rev. Sci. Instrum.* **1998**, *69*, 4002.

(77) Zhang, R.; Lei, W.; Molina, L.T.; Molina, M.J. *Int. J. Mass Spectrom. Ion Proc.*, **2000**, *194*, 41.

(78) Lovejoy, E.R.; Murrells, T.P.; Ravishankara, A.R.; Howard, C.J. *J. Phys. Chem.* **1990**, *94*, 2386.

(79) Huey, L.G.; Hanson, D.R.; Howard, C.J. *J. Phys. Chem.* **1995**, 99, 5001.

(80) Walker, R. E.; de Haas, N.; Westenberg, A. A. *J. Chem Phys.* **1960**, *32*, 1314.

(81) Brown, R.L. *J. Res. Natl. Bur. Stand. (U.S.)* **1978**, *83*, 1.

(82) Keyser, L.F. *J. Phys. Chem.* **1984**, *88*, 4750.

(83) Lei, W.; A. Derecskei-Kovacs; Zhang, R. unpublished results. 2000.

(84) Harrison, A.G. *Chemical Ionization Mass Spectrometry*, 2nd ed.; CRC Press: Boca Raton, FL, 1992.

(85) Atkinson R. *J. Phys. Chem. Ref. Data. Monogr.* **1994**, *2*, 1

(86) Morgan, M.E.; Pilling, M.J.; Tulloch, J.M.; Ruiz, R.P.; Bayes, K.D. *J. Chem. Soc. Faraday Trans.* **1982**, *78*, 1323.

(87) Jenkin, M.E.; Murrells, T.P.; Shalliker, S.J.; Hayman, G.D. *J. Chem. Soc. Faraday Trans.* **1993**, *89*, 433.

(88) Troe, J. *J. Chem. Phys.* **1977**, *66*, 4745.

(89) Myers T. L.; Forde, N. R.; Hu, B.; Kitchen, D. C.; Butler, L. J. *J. Chem. Phys.* **1997**, *107*, 5361.

(90) Since the rates of reaction and collisional deactivation for isoprene + O(1D) are not known, we have used values pf 2.0 x 10-10 cm3 molecule-1 s-1 to describe both processes, which are consistent with rates of reaction and deactivation for O(1D) with other large hydrocarbons; Michaud, P.; Paraskevopoulos, G.; Cvetanovic, R. J. *J. Phys. Chem.* **1974**, *78*, 1457.

(91) Jacobs, A.; Klainermans, K.; Kuge, H.; Wolfrum, J. *J. Chem. Phys.* **1983**, *79*, 3162.

(92) Luque, J.; Crosley, D. R., "LIFBASE : Database and Spectra; Simulation Program (Version 1.5)", SRI International Report, MP99-009, 1999.

(93) McGivern, W. S.; Suh, I.; Clinkenbeard, A.; Zhang, R.; North, S. *J. Phys. Chem.*
      2000, *104,* 6609.

(94) Gilbert, R. G.; Smith, S. G. *Theory of Unimolecular and Recombination Reactions*;
      Blackwell Scientific: Oxford, U.K. 1990.

VITA

Inseon Suh was born in Pusan, Korea on 27 September 1973. She received her high school diploma from the Hanyang Girl's School in Seoul, Korea in February of 1992. In February of 1996, she received a B.S. in Chemistry from Seoul Women's University. She began her M.S. program at Texas A&M University in August of 1998. Following graduation, she plans to pursue her Ph.D program at Texas A&M University.

The author's permanent mailing address is:

2402 Samsung Omni-Tower, Sindeabang 2

Dongjak-gu, Seoul, Korea 156-012